Decoding pelagic ciliate (~~Protozoa,~~ Ciliophora) community divergences in size spectrum, biodiversity and driving factors spanning global five temperature zones

Chaofeng Wang[1,2,3,4], Zhiqiang Xu[1,5], Guangfu Luo[6], Xiaoyu Wang[7], Yan He[8], Musheng Lan[6], Tiancheng Zhang[2], Wuchang Zhang[1,3,4]

[1]CAS Key Laboratory of Marine Ecology and Environmental Sciences, Institute of Oceanology, Chinese Academy of Sciences, Qingdao, 266071, China
[2]State Key Laboratory of Mariculture Breeding, Key Laboratory of Marine Biotechnology of Fujian Province, Institute of Oceanology, College of Marine Sciences, Fujian Agriculture and Forestry University, Fuzhou, 350002, China
[3]Laboratory for Marine Ecology and Environmental Science, Qingdao National Laboratory for Marine Science and Technology, Qingdao, 266237, China
[4]Center for Ocean Mega-Science, Chinese Academy of Sciences, Qingdao, 266071, China
[5]Jiaozhou Bay Marine Ecosystem Research Station, Institute of Oceanology, Chinese Academy of Sciences, Qingdao, 266071, China
[6]Polar Research Institute of China, Shanghai, 200136, China
[7]Frontiers Science Center for Deep Ocean Multispheres and Earth System, Key Laboratory of Physical Oceanography, Ocean University of China, Qingdao 266100, China
[8]First Institute of Oceanography and Key Laboratory of Marine Science and Numerical Modeling, Ministry of Natural Resources, Qingdao, 266061, China

Correspondence to: Chaofeng Wang (wangchaofeng@qdio.ac.cn); Wuchang Zhang (wuchangzhang@qdio.ac.cn)

Abstract. The c~~C~~ommunity structure of microzooplanktonic ciliate~~s~~ ~~–~~ encompassing ~~in~~ size spectrum, biodiversity and biotic-abiotic interplay ~~–~~ are critical~~essential components~~ for unravelling their ecological role in marine ecosystems, yet remain challenging to elucidate on a global scale. To address this knowledge gap, we conducted field observational studies across five temperature zones (North Frigid Zone, NFZ; Sub-Arctic Zone, SAZ; North Temperate Zone, NTZ; Torrid Zone, TZ; South Frigid Zone, SFZ). Our analysis demonstrate ~~revealed that~~ a sharp~~ly~~ decline in ciliate abundance and biomass ~~occurred at~~below the 100 m layer, with distinct vertical distribution patterns observed in each climate region. Moreover, ciliate size spectra exhibited a decrease trend from small to large size spectra, with steeper slopes observed in bipolar zones (NFZ and SFZ) ~~the NFZ and SFZ~~ compared to the other temperature zones. Latitudinally,~~Furthermore,~~ ~~an anti-phase relationship between~~ ciliate abundance and tintinnid biodiversity exhibited an anti-phase relationship,~~was observed in latitudinal direction, with~~ where the TZ hosted peak biodiversity while bipolar seas showed the highest abundance.~~and bipolar seas characterized by the highest biodiversity and abundance, respectively.~~ Moreover, a multivariate biota-environment analysis indicated that temperature exert a primary influence on ~~microzooplanktonic~~ ciliate community constitution~~s~~ in the global marine ecosystem, and the bottom-up control play a key role in shaping ~~ciliate~~ assemblages~~community~~. In conclusion, these results underscore the unprecedented divergences in ciliate trait structure

among five temperature zones and can be generalised for assessing the potential effects of climate change on pelagic microzooplankton in future marine realm.

1 Introduction

The Earth is traditionally partitioned~~divided~~ into five temperature zones based on established climate classifications: the North Frigid Zone (NFZ), North Temperate Zone (NTZ), Torrid Zone (TZ), South Temperate Zone (STZ), and South Frigid Zone (SFZ) (Köppen 1936; Trewartha et al. 1967). Therein, each temperature zone possessed unique ocean circulation pattern and concurrent specific plankton biome structures (Longhurst 2007; Spalding et al. 2012). Albeit a myriad of prevailing research relevant to plankton biogeography and its interplay with environmental drivers highlighting its importance in disentangling marine ecosystems and biogeochemical cycles (e.g., Wang et al. 2020; Darnis et al. 2022; Segaran et al. 2023; Tagliabue et al. 2023), substantial global-scale studies have predominantly relied on modeling frameworks~~were conducted through diverse modeling approaches~~ (Spalding et al. 2012; Blanchard et al. 2017; Anderson et al. 2021; Benedetti et al. 2021; Heneghan et al. 2023; Atkinson et al. 2024). To date, an explicit and comprehensive representation of plankton community trait structure using data-derived statistical analysis originated from field-surveys remains unresolved.

A holistic paradigm of plankton biogeography across marine ecosystem is crucial for deciphering global ecological connectivity (Hillman et al. 2018) and predicting how ecosystems respond to stressors induced by climate change (Darnis et al. 2022). Over recent decades, anthropogenic CO_2 emissions have led to increased atmospheric concentrations and greater global radiative forcing (Tagliabue et al. 2023), triggering diverse ecological feedbacks worldwide, for instance poleward distribution shifts (Neukermans et al. 2018; Oziel et al. 2020; Benedetti et al. 2021), adjustments in phenology (Poloczanska et al. 2013; Atkinson et al. 2015; Chust et al. 2024), and reductions in mean body size (Daufresne et al. 2009; Verberk et al. 2021; Wang et al. 2023a, 2023b). In this sense, extensive existing studies put emphasis on biotic community response to climate change in the bipolar and adjacent seas owing to their higher susceptibility compared to tropical, subtropical, and temperate seas (Serreze et al. 2009; Screen and Simmonds 2010; IPCC 2023; Noh et al. 2024). Unfortunately, an informative research relate to environmental affinity of plankton, particularly microzooplankton, is not sufficiently understood in aforementioned five temperature zones.

带格式的: 下标

In the realm of microzooplankton, pelagic ciliates stand out as the predominant biological entities, spanning in size from 10 to 200 μm, and hold significant sway over both biodiversity and abundance, particularly in the polar and adjacent seas (Taniguchi 1984; Strom and Fredrickson 2008; Lu and Weisse 2022; Kohlbach et al. 2023; Wang et al. 2023a, 2024a, 2024b). Taxonomically categorized within the phylum Ciliophora, class Spirotrichea, and subclasses Oligotrichia and Choreotrichia, pelagic ciliates, including aloricate ciliates and tintinnids, are ubiquitous single-cell protozoans found in various aquatic environments worldwide (Lynn 2008). Furthermore, ciliates play an irreplaceable role in marine trophodynamics (carbon cycle and energy transfer) through prey-predator interactions, serving as both phytoplankton grazers and prey for metazoans (Stoecker et al. 1987; Dolan et al. 1999; Calbet and Saiz 2005; Gómez 2007; Weisse and Sonntag 2016). Specifically, owing to their simple life cycle, fast-reaction to environmental changes, and strong adaptability, pelagic ciliates, particularly tintinnids, are widely recognized as ideal bioindicators for assessing various sea conditions (e.g., Kato and Taniguchi 1993; Jiang et al. 2013; Wang et al. 2021; Yu et al. 2022).

Recent escalation in global warming have imposed a cascade of impacts on aquatic ecosystems, presenting a formidable challenge to inherent holopelagic species that project the relevant adaptative strategies (Stabeno et al. 2012; Yasumiishi et al. 2020; Carvalho et al. 2021; Atkinson et al. 2024). Accordingly, a prevailing viewpoint for phytoplankton, the cornerstone of marine pelagic food web, is a major decline in both biomass and size spectra in the NTZ, TZ and STZ (Li et al. 2009; Lotze et al. 2019; Tittensor et al. 2021), leading to subsequent declines for higher trophic levels, termed “trophic amplification” (Kwiatkowski et al. 2019; du Pontavice et al. 2021). As grazer of pelagic phytoplankton, response of microzooplanktonic ciliates to ocean warming in the bipolar and adjacent seas is substantial (Li et al. 2022; Wang et al. 2022a, 2023a, 2023b, 2024b), yet comparative assessments amid their trait structure (e.g., size spectra, biodiversity and biotic-abiotic interplay) remain unexplored to date.

~~Hence~~Consequently, ~~focusing on~~elucidating microzooplanktonic ciliate size spectra, species diversity and biotic-abiotic interplay ~~in~~ at a global-scale is critical for projecting future marine ecosystem dynamics, particularly given their unresolved role in plankton response to sophisticated climate changes. Here, ~~for future marine ecosystem dynamic projections could bolster our understanding of plankton response to sophisticated climate changes, particularly as the underlying microbial processes remain poorly resolved. Here,~~ we propose a hypothesis that hydrographic variability~~variations in hydrographic conditions~~ are likely responsible for the observed divergence ~~diverse~~ in global ciliate trait structures ~~observed globally~~. By optimizing f~~ei~~ield observational data and available methods, this study aims to: (1)~~our objective is two-fold: disclose~~ decode adaptative strategies of ~~the~~ microzooplanktonic ciliate ~~adaptative strategies~~ to heterogeneous hydrographic conditions~~alien hydrography among~~ across temperature zones~~;~~, and (2) evaluate their potential response dynamics ~~of microzooplankton~~ to accelerating~~rapid~~ climate change. Given the current foreseeable rapid climate change process, this study will offer a valuable norm for facilitating the phenological and bioclimatic progression of microzooplankton shifts in future global marine ecosystem realm.

2 Materials and Methods

2.1 Study area and field sampling

Based on their latitudinal locations, field samplings of microzooplanktonic ciliates were conducted in five temperature zones (Trewartha et al. 1967): 1, North Frigid Zone (NFZ), encompassing the Arctic Ocean, during July to August 2019 and 2023 aboard the *R.V.* “Xiangyanghong ~~0~~1” and *R.V.* “Xuelong 2”, respectively; 2, the Sub-Arctic Zone (SAZ), located in the Bering Sea, in July to August 2019 aboard the *R.V.* “Xiangyanghong ~~0~~1”; 3, the North Temperate Zone (NTZ), situated in the North Pacific, in September 2019 aboard the *R.V.* “Dongfanghong 3”; 4, the Torrid Zone (TZ), which includes the tropical western Pacific in December 2016 and August 2017 aboard the *R.V.* “Kexue”, and the Indian Ocean in March 2021 aboard the *R.V.* “Xiangyanghong ~~10~~6”; and 5, the South Frigid Zone (SFZ), covering the Southern Ocean, from December 2020 to March 2021 aboard the *R.V.* “Xuelong 2” (Figure 1). A total of 1117 samples (175 stations along 19 transects) were sampled.

Seawater samples were collected with a rosette sampler carrying 24 Niskin bottles (each 12 L). Simultaneously, environmental factors of sampling depth, temperature, salinity and chlorophyll *a in vivo* fluorescence (Chl *a*) were obtained by a multi-sensor profiler (CTD–SeaBird SBE 911) at each cruise. All microzooplanktonic ciliate samples were collected at seven standardized depth (surface [2 m], 25, 50, 75, 100, 150 and 200 m) at at each designated station, with the exception of SAZ stations where bathymetry limited sampling to depths <200 m. ~~(except the SAZ, where seafloor of most stations were shallower than 200 m) were collected at surface (2 m), 25 m, 50 m, 75 m, 100 m, 150 m and 200 m at each designated station.~~ Furthermore, each sample was fixed with acid Lugol's (1% final concentration) and preserved in darkness at 4 ℃ until ~~further analysis in the~~ laboratory analysis.

带格式的: 字体: Times New Roman

带格式的: 字体: Times New Roman

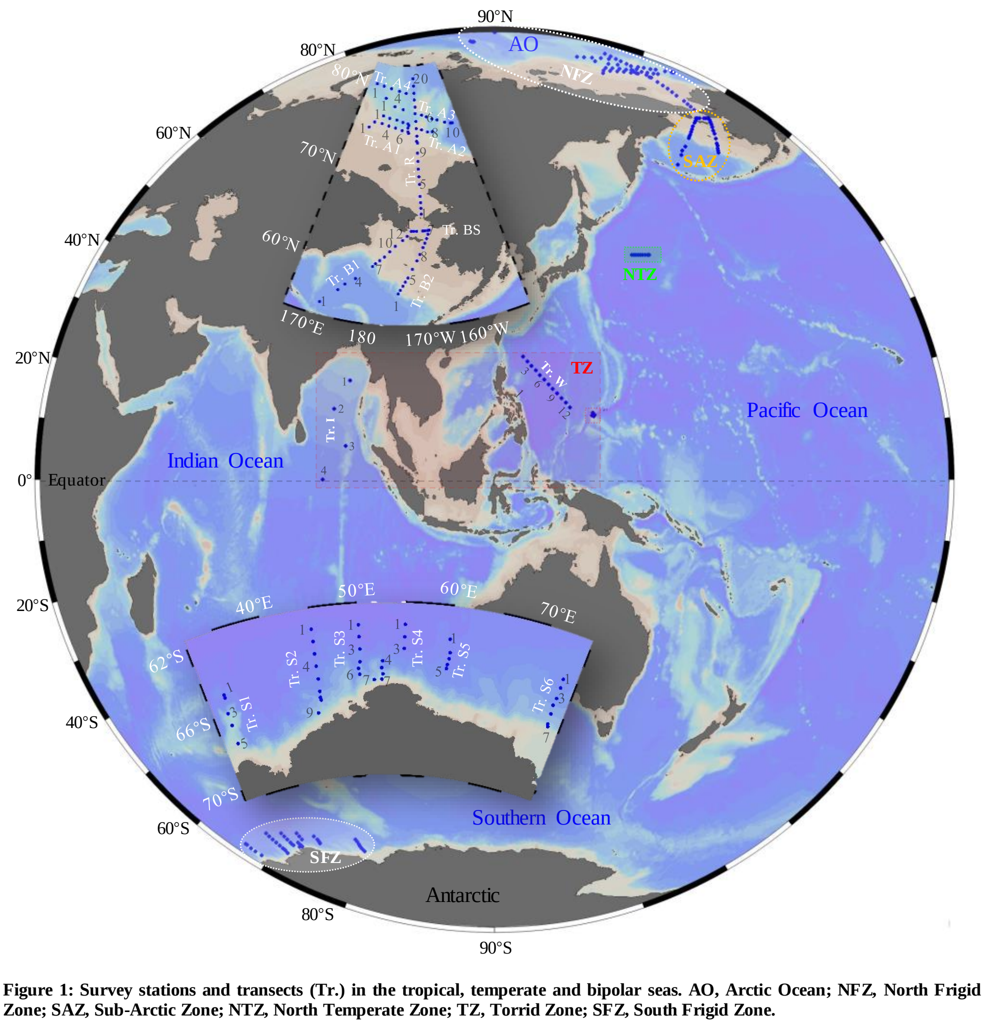

Figure 1: Survey stations and transects (Tr.) in the tropical, temperate and bipolar seas. AO, Arctic Ocean; NFZ, North Frigid Zone; SAZ, Sub-Arctic Zone; NTZ, North Temperate Zone; TZ, Torrid Zone; SFZ, South Frigid Zone.

2.2 Sample analysis

Laboratory processing involved concentrating each sample to approximately 200 mL through siphon-assisted supernatant removal following 60 h sedimentation. In the laboratory, each sample was concentrated to approximately 200 mL by siphoning off supernatant after settling 60 h. After two rounds of siphon process, a final of 25 mL highly concentrated sample was obtained, and then settled in a Utermöhl counting chamber (Utermöhl 1958). Quantitative analysis was performed using an Olympus IX71 inverted microscope (100× or 400× magnification) to enumerate total ciliate abundance (including aloricate ciliates and tintinnids), measure morphometric parameters (body size), and document species richness across all five temperature zones by Chaofeng Wang. To ensure accuracy, Each sample in the chamber was examined using an Olympus IX 71 inverted microscope (100× or 400×), and total abundance, body-size and species richness of ciliates (including aloricate ciliates and tintinnids) were recorded at five temperature zones by Chaofeng Wang. To ensure accuracy, cellular dimensions size (e.g., length, width, shape) of aloricate ciliate or each tintinnid species were measured for at least 10 individuals if possible.

Additionally, body-size of both aloricate ciliates and tintinnids were categorized into 10 μm increments (10–20 μm, 20–30 μm, etc.) based on body length (Wang et al., 2020), and further classified into small (10–20 μm)/medium (20–50 μm)/large (>50 μm) size-fractions following Yang et al. (2019). Regarding species richness, tintinnid identification was assigned to closest species as described in Zhang et al. (2012). Furthermore, we select the average value (15, 25, 35, 45 μm,…, etc) of each size-fraction of both loricate ciliate and tintinnid as the counting criterion for ciliate size spectra (Wang et al. 2024b).

2.3 Data processing

Ciliate volumes were estimated according to their appropriate geometric shapes (cone, ball, cylinder). Carbon biomass of each tintinnid was calculated by the equation (Verity and Lagdon 1984):

$$\mathrm{C} = V_i \times 0.053 + 444.5$$

Where C (10^{-6} μg C) was the carbon biomass of individual tintinnid, V_i (μm^3) was the lorica volume. Additionally, a conversion factor (0.19×10^{-6} μg pg C μm^{-3}) was used for calculating aloricate ciliate carbon biomass (Putt and Stoecker 1989). Concerning Size size spectra biomass, of both ciliate abundance and biomass were classified calculated based their cellular lengthspecific organism volume and conversion equation, then categorized into each size spectrum as in Wang et al. (2024b). Furthermore, in order to better unravelling test tintinnid biodiversity spanning five temperature zones, the Margalef index (d_{Ma}) (Margalef 1958) (1) and Shannon index (H_2') (Shannon 1948) (2) were conducted by the following equations:

$$d_{Ma} = \frac{S-1}{\ln N} \quad (1)$$

where S is the number of species, and N is the total number of tintinnid individuals in the sample.

$$H_2' = -\sum_{i-1}^{S} P_i \, log_2 P_i \quad (2)$$

where S is the number of species, and N is the total abundance of tintinnid individuals in the sample. P_i (N_i/N) is the relative abudnance of i species in a whole community.

带格式的: 字体: (默认) +西文正文 (Times New Roman)

Biogeographically, classification of tintinnid genera (cosmopolitan, warm water, boreal, austral and neritic) was based on Pierce and Turner (1993) and Dolan and Pierce (2013). Among them, tintinnid genera were further classified into oceanic (cosmopolitan, warm water, boreal and austral) and neritic types. Moreover, average value of each parameter was represented as mean ± SD in the following text.

Hereinafter, sampling map was visualized by ODV (Ocean Data View, Version 4.7), and ciliate distributional data of size–diversity and temperature~~—~~diversity relationships were analyzed using Surfer (Version 13.0), Grapher (Version 12.0), and OriginPro 2021 (Version 9.6). Moreover, the Biota-Environment analysis was performed based on Spearman's correlation between log-transformed abiotic parameters and square root-transformed abundance data (t-test) using both PRIMER (Version 5.0) and OriginPro 2021 (Version 9.6). Additionally, the slope of the size spectrum (a straight line fitted through the size spectrum on a log–log plot) (Blanchard et al. 2017) was carried out to quantize its interplay with ciliate abundance at discrete depth of aforementioned global seas (95% confidence). In the following, based on the slope condition, we used the decreasing rate (Δ_D) or increasing rate (Δ_I) according to ciliate abundance or species richness and environmental variables to quantize their interplay in the global seas.

3 Results

3.1 Hydrography and ciliate abundance and biomass

Each environmental parameter (temperature, salinity, and Chl *a*) displayed distinct spatiotemporal variations globally (Figure 2 and Figures S1–~~-~~S3). Horizontally, at surface, 50 and 100 m layers, both temperature and salinity peaked in the Torrid Zone (TZ), contrasting with Chl *a*, which exhibited its lowest value in the same region (Figure 2 and Figures S1–~~-~~S2). At 200 m depth, temperature peaked in the TZ and Chl *a* ~~peaked in the TZ and~~peaked in the North Frigid Zone (NFZ), ~~respectively,~~ contrasting with salinity patterns, which displayed high values in both the TZ and NFZ~~deviating from salinity patterns, which exhibited high values in both the TZ and NFZ~~ (Figure 2 and Figure S1). Vertically, both temperature and Chl *a* declined in the NFZ and Sub-Arctic Zone (SAZ) (surface-peak pattern), while salinity increased from the surface to 200 m layers across all regions (Figures S1–~~-~~S3). Moreover, temperature displayed a low–high–low ~~"sandwich"~~ structure~~ (low–high–low values)~~ at inner stations of the South Frigid Zone (SFZ), and Chl *a* peaked at subsurface layers in both the North Temperate Zone (NTZ) and TZ (Figures S1~~ and S3~~).

Pelagic ciliate abundance ranged from 22–9142 ind. L^{-1} in the NFZ, 182–9242 ind. L^{-1} in the SAZ, 65–886 ind. L^{-1} in the NTZ, 25–436 ind. L^{-1} in the TZ, and 44–5866 ind. L^{-1} in the SFZ, whereas their biomass ranged from 0.0–39.3 μg C L^{-1}, 0.3–24.0 μg C L^{-1}, 0.1–1.1 μg C L^{-1}, 0.0–1.1 μg C L^{-1}, and 0.0–26.1 μg C L^{-1} in aforementioned regions, respectively (Figure 2 and Figures S1–~~-~~S3). Horizontally, both high abundance (≥ 2000 ind. L^{-1}) and biomass (≥ 5.0 μg C L^{-1}) of ciliates were observed in surface layers of the NFZ, SAZ, and SFZ, coinciding with high Chl *a* levels. At 50 m, 100 m and 200 m layers, the SAZ and TZ had the highest and lowest abundance, respectively (Figure 2 and Figure S1). Vertically, both ciliate abundance and biomass exhibited a surface-peak pattern in the NFZ, SAZ, and SFZ, whereas in the NTZ and TZ, this pattern transitioned to subsurface-peak and bimodal-peak distributions, respectively (Figures S1~~ and S3~~S2).

Meanwhile, aloricate ciliates dominated the ciliate community, accounting for ≥ 90% of total abundance at each depth in the NFZ, NTZ, TZ, and SFZ. However, in the SAZ, tintinnid played a more significant role in the ciliate community, with an average relative abundance at most sampling depths exceeding 10% (Figures S4). In terms of aloricate ciliates in the horizontal direction, small (10–20 μm) and medium (20–50 μm) size-fractions in the SAZ exhibited the highest average abundance at surface, 50 m, 100 m, and 200 m layers, whilst the largest (> 50 μm) size-fraction had the highest average abundance at the surface, 50 m, and 100 m layers in the SFZ (Figures S5). Additionally, except for the NTZ, the abundance and relative abundance of the medium size-fraction were highest in the other four regions at both the surface and 50 m layers. At 200 m depth, the small size-fraction predominated among the aloricate ciliates (Figures S5). Vertically, the relative abundance of the large size-fraction (>50 μm) exhibited a decreasing trend, whereas the small size-fraction displayed an increasing trend across the five temperature zones~~the large (> 50 μm) and small size-fractions exhibited an inverse distribution characteristic across five temperature zones~~ (Figures S5).

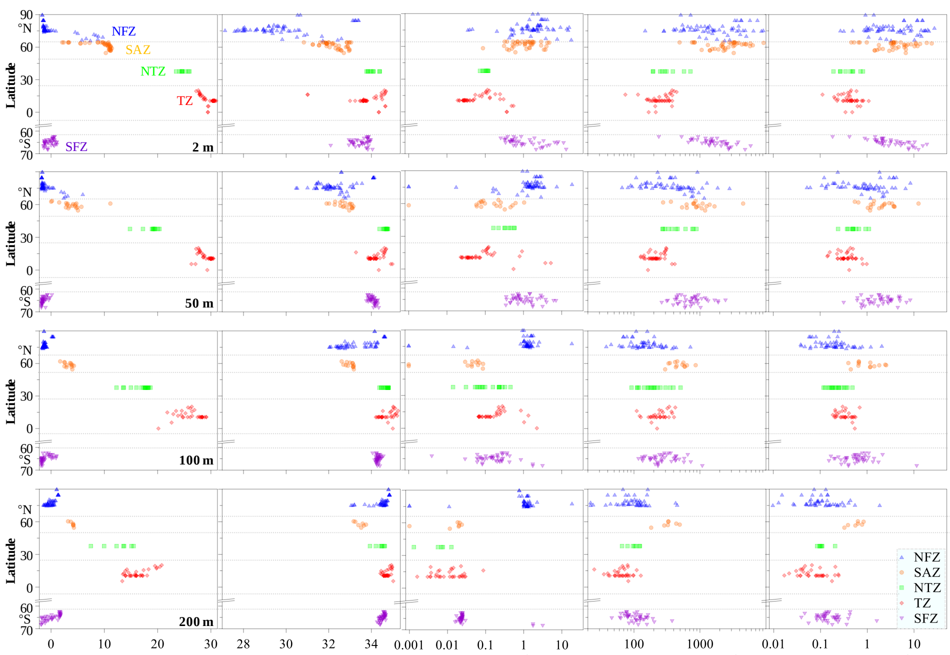

Figure 2: Variations in environmental variables and ciliate abundance and biomass at discrete depth in each temperature zone~~in the North Frigid Zone (NFZ), sub-Arctic Zone (SAZ), North Temperate Zone (NTZ), Torrid Zone (TZ) and South Frigid Zone (SFZ)~~.

3.2 Notable variations in pelagic ciliate size spectrum composition

The abundance and biomass of pelagic ciliate size spectra displayed significant variations across global seas (95% confidence) (Figures 3–4). Generally, the slopes of the normalized abundance and biomass size spectra varied from -2.13 to -0.87 (average -1.60 ±0.33), and from -0.99 to -0.08 (average -0.53 ±0.25), respectively, with the former was much steeper than ~~tha~~ the latter (Figure 3). Therein, ciliate abundance decreased from small (15 μm) to large size spectra (> 100 μm), with the slopes of the normalized abundance size spectra in both the NFZ (-2.13 to -1.93, average -2.01 ±0.09) and SFZ (-2.01 to -1.63, average -1.80 ±0.17) being steeper than in the other three regions at each depth (Figure 3~~a~~). Additionally, a secondary peak in abundance, featuring large size spectra (> 100 μm), was observed at the surface layers of the NFZ, SAZ, and SFZ (Figure 3~~a~~).

In contrast, the distribution characteristics of ciliate biomass within size spectra did not align with the abundance trend (Figure ~~3~~4~~b~~). Notably, the 65 μm size spectrum exhibited the highest values at both surface and 50 m layers of the NFZ, followed by the SFZ (55 μm) and SAZ (55 μm), with the TZ (35 μm) and NTZ (25 μm) showing lower values (Figure ~~3~~4~~b~~). Moreover, the slopes of the normalized biomass size spectra in the SFZ (-0.99 to -0.77, average -0.86 ±0.10) were steeper than that in the SAZ (-0.74 to -0.43, average -0.62 ±0.13), NTZ (-0.63 to -0.44, average -0.53 ±0.09), TZ (-0.74 to -0.25, average -0.47 ±0.22) and NFZ (-0.37 to -0.08, average -0.21 ±0.12) (Figure ~~3~~4~~b~~). Interestingly, the highest biomass of ciliate size spectra at the surface, 50 m, and 100 m layers of the TZ corresponded to the 35 μm size spectrum, while at the 200 m layer, the 15 μm size spectrum became dominant (Figure ~~3~~4~~b~~).

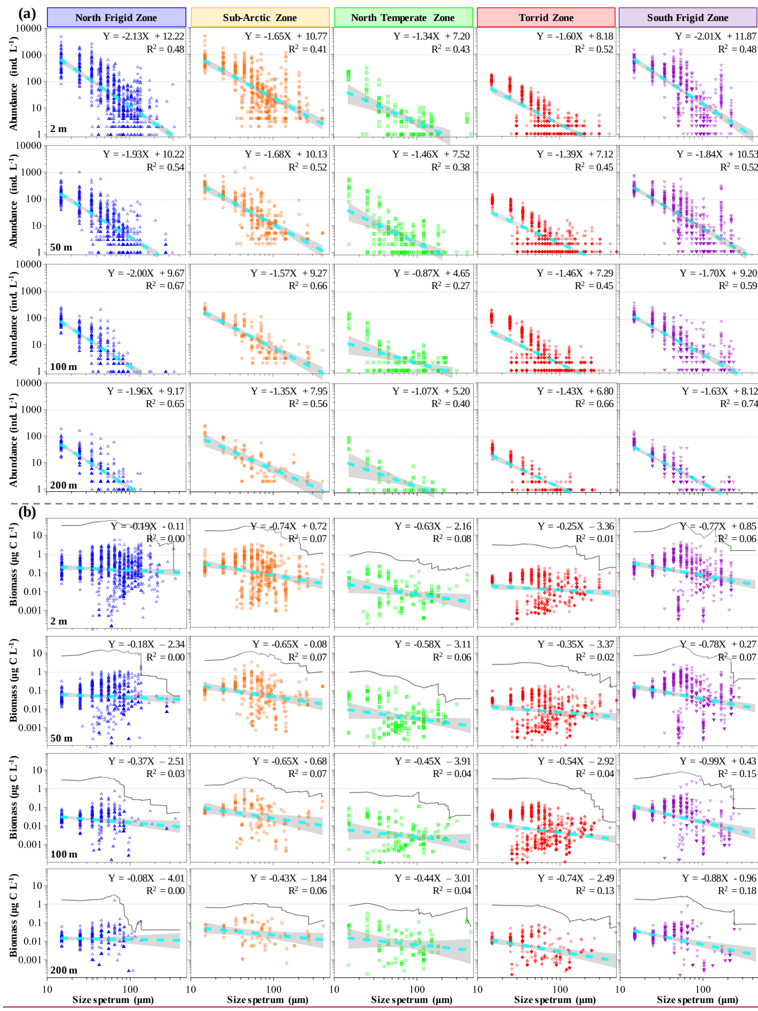

(a)
North Frigid Zone
Sub-Arctic Zone
North Temperate Zone
Torrid Zone
South Frigid Zone
Abundance (ind. L-1)
Y = -2.13X + 12.22 R2 = 0.48
Y = -1.65X + 10.77 R2 = 0.41
Y = -1.34X + 7.20 R2 = 0.43
Y = -1.60X + 8.18 R2 = 0.52
Y = -2.01X + 11.87 R2 = 0.48
2 m
Y = -1.93X + 10.22 R2 = 0.54
Y = -1.68X + 10.13 R2 = 0.52
Y = -1.46X + 7.52 R2 = 0.38
Y = -1.39X + 7.12 R2 = 0.45
Y = -1.84X + 10.53 R2 = 0.52
50 m
Y = -2.00X + 9.67 R2 = 0.67
Y = -1.57X + 9.27 R2 = 0.66
Y = -0.87X + 4.65 R2 = 0.27
Y = -1.46X + 7.29 R2 = 0.45
Y = -1.70X + 9.20 R2 = 0.59
100 m
Y = -1.96X + 9.17 R2 = 0.65
Y = -1.35X + 7.95 R2 = 0.56
Y = -1.07X + 5.20 R2 = 0.40
Y = -1.43X + 6.80 R2 = 0.66
Y = -1.63X + 8.12 R2 = 0.74
200 m
(b)
Biomass (μg C L-1)
Y = -0.19X - 0.11 R2 = 0.00
Y = -0.74X + 0.72 R2 = 0.07
Y = -0.63X – 2.16 R2 = 0.08
Y = -0.25X – 3.36 R2 = 0.01
Y = -0.77X + 0.85 R2 = 0.06
2 m
Y = -0.18X – 2.34 R2 = 0.00
Y = -0.65X - 0.08 R2 = 0.07
Y = -0.58X – 3.11 R2 = 0.06
Y = -0.35X – 3.37 R2 = 0.02
Y = -0.78X + 0.27 R2 = 0.07
50 m
Y = -0.37X – 2.51 R2 = 0.03
Y = -0.65X - 0.68 R2 = 0.07
Y = -0.45X – 3.91 R2 = 0.04
Y = -0.54X – 2.92 R2 = 0.04
Y = -0.99X + 0.43 R2 = 0.15
100 m
Y = -0.08X – 4.01 R2 = 0.00
Y = -0.43X – 1.84 R2 = 0.06
Y = -0.44X – 3.01 R2 = 0.04
Y = -0.74X – 2.49 R2 = 0.13
Y = -0.88X - 0.96 R2 = 0.18
200 m
Size spetrum (μm)

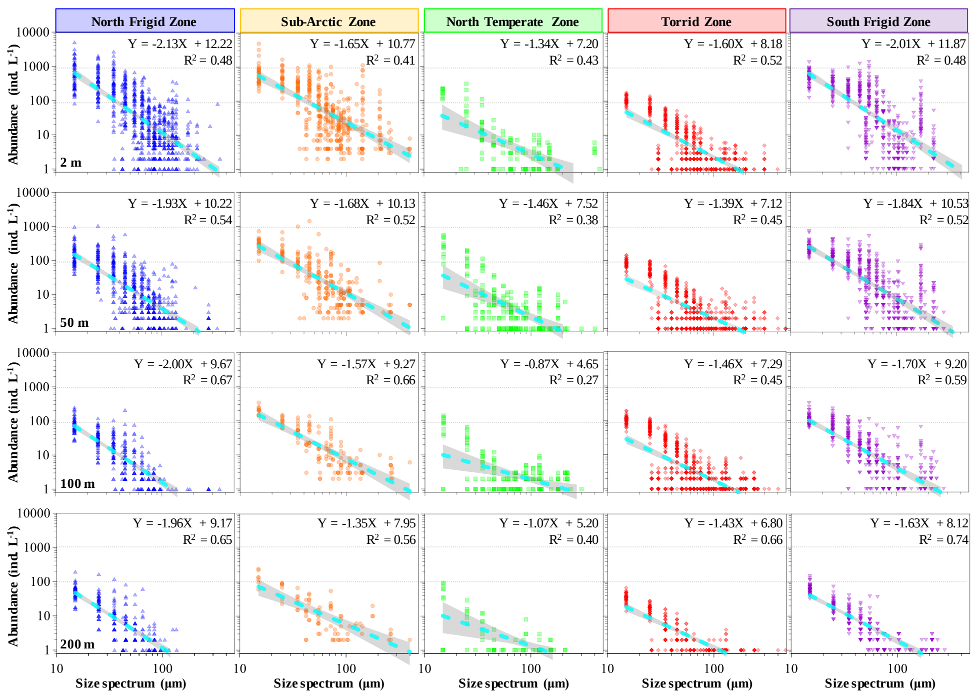

Figure 3: Variations in body-size spectra of ciliate normalized abundance ~~(a) and biomass (b)~~ at discrete depth in each temperature zone.

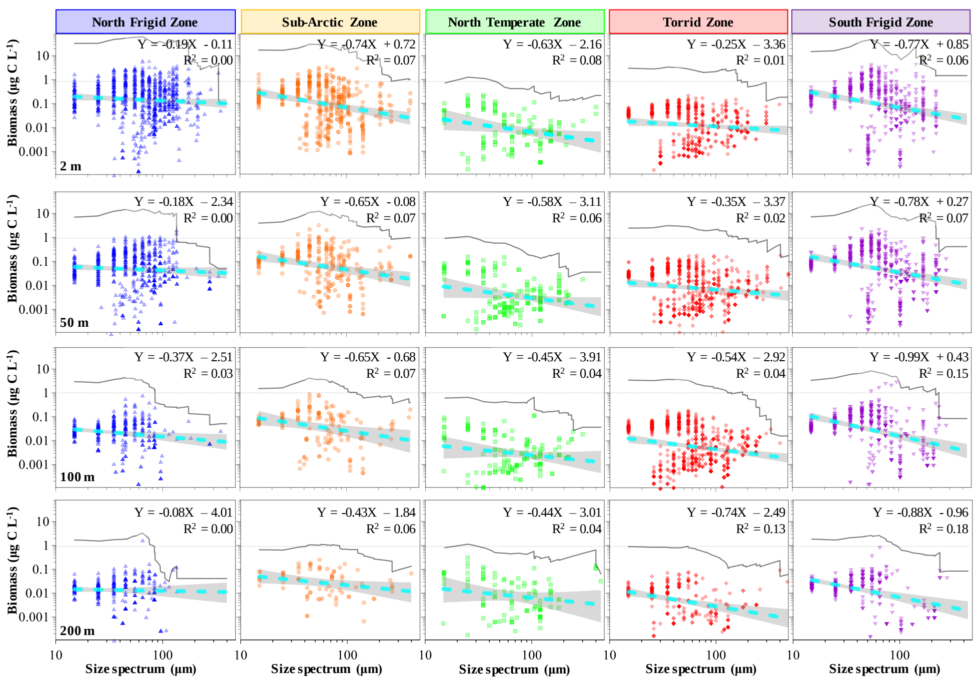

Figure 4: Variations in body–size spectra of ciliate normalized biomass at discrete depth in each temperature zone.

3.3 Dynamics in tintinnid species richness and diversity indices

Tintinnid assemblages exhibited significant spatial heterogeneity in both species richness and diversity metrics (Margalef index–d_{Ma}, Shannon index–H_2')~~Tintinnid species richness and diversity indices exhibited obvious variations in both horizontal and vertical distributions spanning five temperature zones~~ across five temperature zones (Figure ~~4~~ 5 and Figure S6). Horizontally, species richness, Margalef index (d_{Ma}) and Shannon index (H_2') were notably high at discrete layers in both the NTZ and TZ, followed by the SAZ, NFZ, and SFZ (Figure ~~4a~~ 5a and Figure S6). To enable cross-regional comparison, we excluded neritic genera (restricted to SAZ and NFZ) from species richness calculations, revealing higher species richness in the SFZ versus NFZ (Figure 5a). ~~Given that neritic genera were only present in the SAZ and NFZ, species richness excluding neritic genera was also examined to maintain consistency with the other three regions, revealing higher species richness in the SFZ compared to the NFZ (Figure 4a).~~ Vertically, elevated values of tintinnid species richness, d_{Ma} ~~dMa~~ and H_2'~~H2'~~ were primarily observed in the upper 50 m waters of the NFZ, SAZ, and SFZ, while these values peaked at 75 m and 100 m in the NTZ and TZ, respectively (95% confidence) (Figure ~~4b~~5b). Notably, we observed an

带格式的: 正文

inverse relationship between ciliate abundance and tintinnid species richness across five temperature zones (Figure S7), suggesting potential competitive exclusion or niche partitioning dynamics. Furthermore, an analysis of the relationship between ciliate abundance and species richness revealed that regions characterized by high ciliate abundance were often accompanied by low tintinnid species richness (Figure S7).

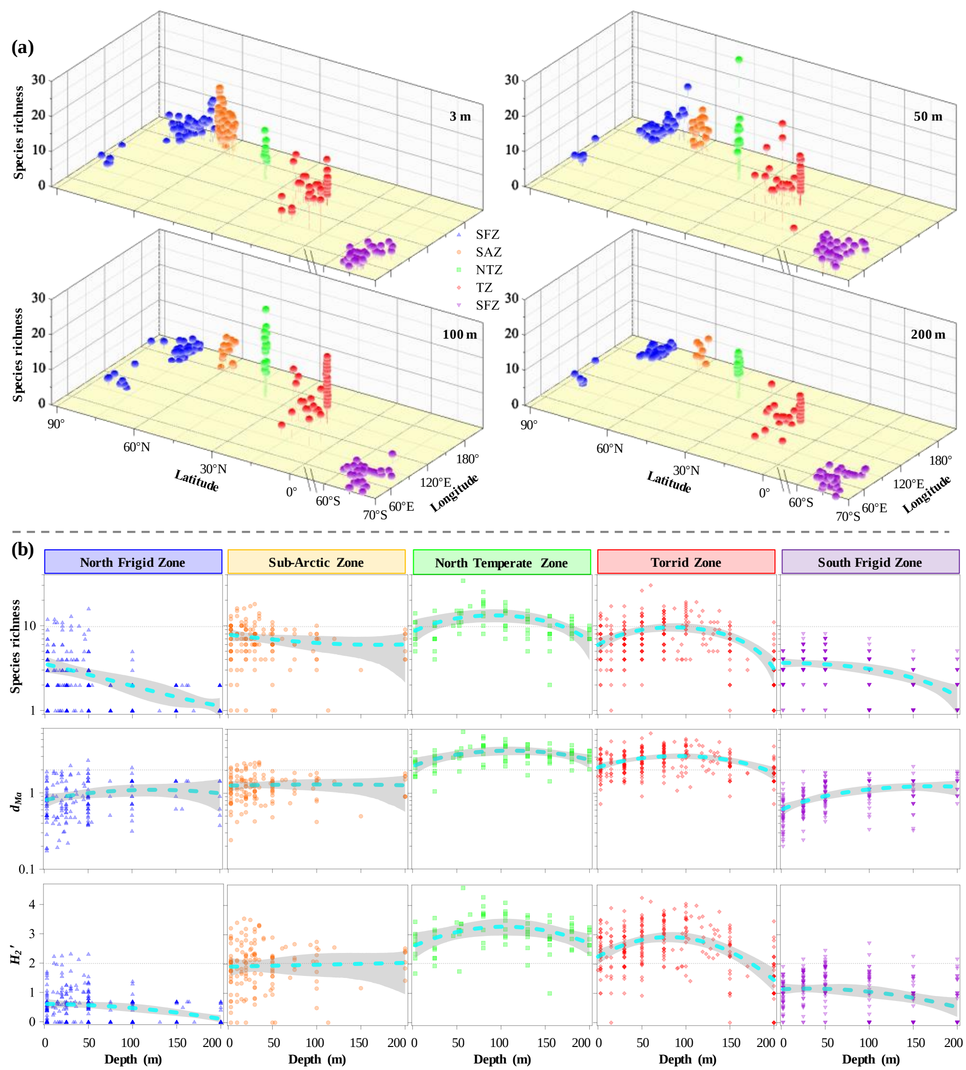

Figure 45: Variations of tintinnid species richness, Margalef index (d_{Ma}) and Shannon index (H_2') in latitudinal (a) and vertical (b) direction of all regions.

3.4 Biotic-abiotic interplay and its variations

Ciliate abundance and tintinnid species richness exhibited varying correlations with environmental parameters across the five temperature zones (Figure~~s~~ ~~5–7~~6 and Figures S8–S10). In terms of the biotic-abiotic interplay trend, our results revealed that only the NFZ and SAZ exhibited an increasing trend ($\Delta_I \geq 0.03$) in abundance–temperature correlation at both surface and 50 m layers compared to other three temperate zones (Figure ~~5a~~ S9). Concerning all sampling layers, only the SFZ, differing from the trends observed in the other four temperature zones, displayed a decrease in ciliate abundance with increasing temperature (Δ_D = -0.26, R^2 = 0.06) (Figure ~~S8~~S10). Moreover, only the TZ and SFZ exhibited an increase ($\Delta_I \geq 0.29$) and a decrease ($\Delta_D \leq -0.01$) trend at each sampling layer in abundance–salinity correlation, respectively (Figure ~~5b~~6b). Furthermore, only SFZ showed an increase ($\Delta_I \geq 0.02$) trend at each sampling layer in abundance–Chl *a* correlation (Figure S8~~5c~~), which was align with trends in other four temperature zones at all sampling layers ($\Delta_I \geq 0.06$) (Figure ~~S8~~S10).
Regarding species richness–temperature correlation, the highest increasing trend occurred at 50 m of the NFZ (Δ_I = 0.26, R^2 = 0.44), while the highest decreasing trend was found at 100 m of the SAZ (Δ_D = -0.28, R^2 = 0.09) (Figure S9~~6a~~). As for all sampling layers, only the NFZ and TZ exhibited an increasing trend in species richness–temperature correlations, with the former (Δ_I = 0.15, R^2 = 0.26) being higher than the latter (Δ_I = 0.06, R^2 = 0.23) (Figure ~~S8~~S10). Moreover, concerning biotic–salinity correlations, only the SAZ exhibited an increase ($\Delta_I \geq 0.06$) trend at each sampling layer (Figure S9~~6b~~). ~~At all sampling layers, contrasting with decrease trend in abundance-salinity correlation in each temperature zone, the increase trends in species richness-salinity correlations were observed in the NTZ (Δ_I = 0.45, R^2 = 0.08) and SAZ (Δ_I = 0.20, R^2 = 0.03) (Figure S8). Furthermore~~In addition, only the bipolar seas exhibited an increasing trend ($\Delta I \geq 0.01$) in species richness–-Chl *a* correlation at each sampling layer (Figure S9~~6c~~). ~~Simultaneously, species richness exhibited an increasing trend in their correlation with Chl a at all sampling layers of the SAZ (Δ_I = 0.05, R^2 = 0.02), NTZ (Δ_I = 0.07, R^2 = 0.05) and TZ (Δ_I = 0.20, R^2 = 0.15) (Figure S8).~~
To further quantize the physical-biological interplay in five temperature zones, we conducted both principal component analysis (PCA) and spearman's rank correlation via using abundance of aloricate ciliate, tintinnid and total ciliate, and tintinnid species richness to test abiotic influence (Figure ~~7~~6). The PCA revealed that two principal components effectively differentiated the environmental conditions among five temperature zones. These components accounted for a substantial proportion of the biotic variation in the NFZ (62.85%), SAZ (67.83%), NTZ (64.75%), TZ (72.68%), SFZ (63.84%) and all regions (61.42%) (Figure ~~7a~~6a). Akin to PCA, spearman's rank correlation reflected that abundance of aloricate ciliate, tintinnid and total ciliate in all five temperature zones displayed a strong significant negative and positive correlation with depth ($p < 0.01$) and Chl *a* ($p < 0.01$), respectively (Figure ~~7b~~6b). Furthermore, both aloricate ciliate and tintinnid featured significant positive correlation with temperature in the SAZ, NTZ and TZ ($p < 0.05$). However, in the SFZ, relationship between aloricate ciliate and temperature shifted to a significant negative correlation ($p < 0.05$) (Figure ~~7b~~6b). Except that, tintinnid species richness exhibited strong significant negative correlation with salinity in both the NFZ and SFZ ($p < 0.01$),

带格式的: 上标

带格式的: 字体: 倾斜

which was unconsistent with that in the NTZ, where changed into strong significant positive correlation (p < 0.01) (Figure 7b6b).

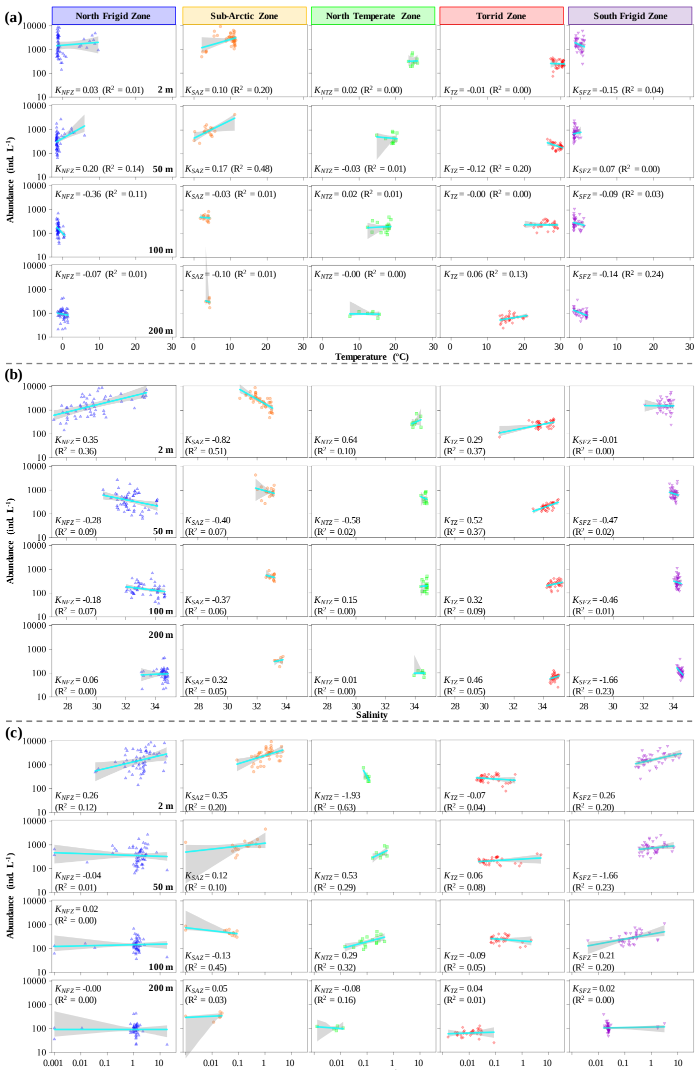

Figure 5: Variations in slopes between ciliate abundance and environmental variables (temperature, salinity, Chl *a*) at discrete depth in each temperature zone.

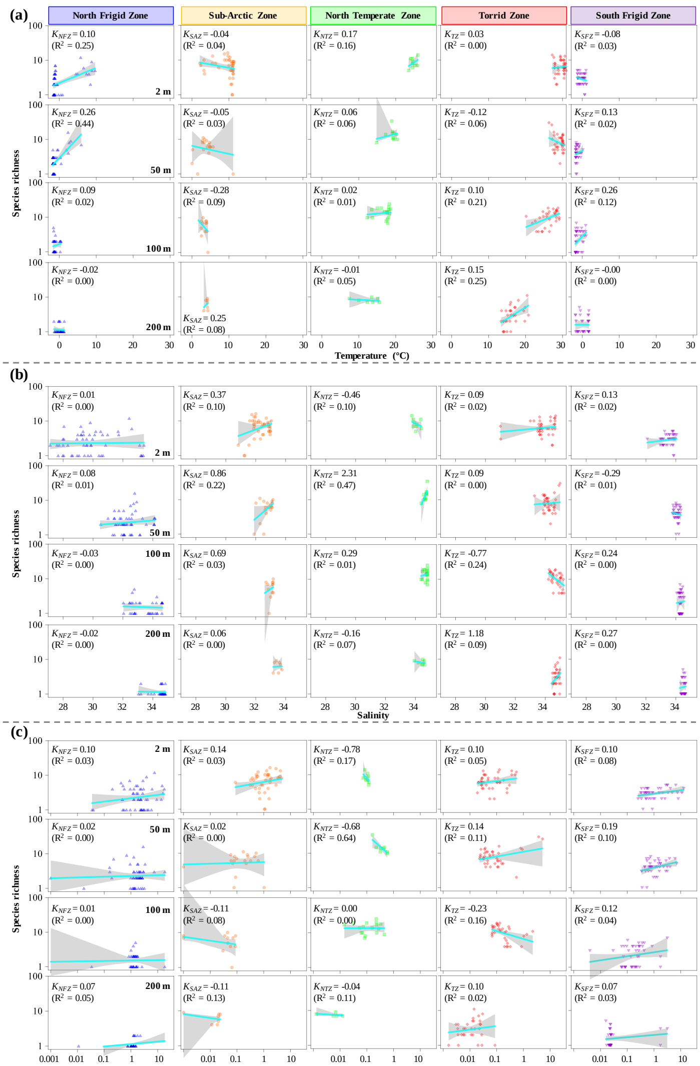

Figure 6: Variations in slopes between tintinnid species richness and environmental variables (temperature, salinity, Chl *a*) at discrete depth in each temperature zone.

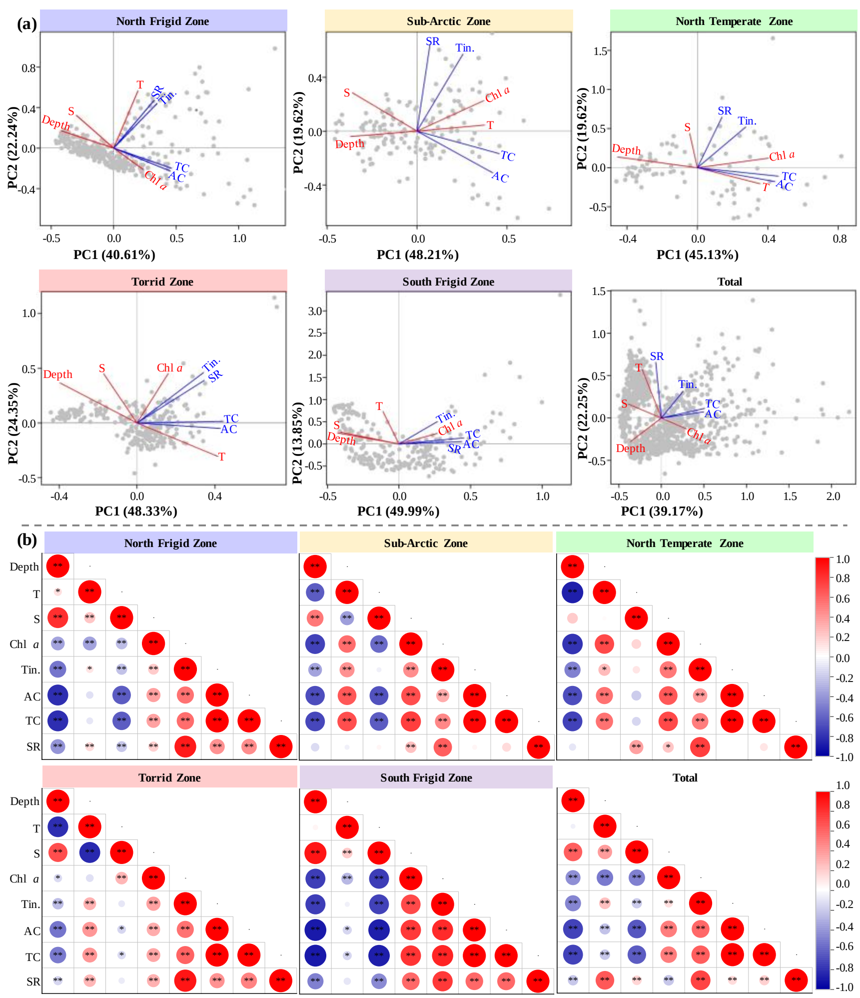

Figure ~~7~~6: Variations in principal component analysis (PCA) (a) and spearman's rank correlation (b) between environmental parameters (Depth; temperature, T; salinity, S; Chl *a*) and ciliate (tintinnid, Tin; aloricate ciliate, AC; total ciliate, TC; tintinnid species richness, SR) in five regions. The *x*-axis is the first PCA axis, and the *y*-axis is the second PCA axis. Environmental variables and ciliates are indicated by red lines and black lines, respectively. Grey dots are sampling points. **: $p < 0.01$, *: $p < 0.05$, t-test.

4 Discussion

In a nutshell, this study presentsprovides a first holistic epitome of microzooplanktonic ciliate community divergences and corresponding biotic–-abiotic interplay among five temperature zones (NFZ, SAZ, NTZ, TZ, SFZ) spanning the global scale, revealing significant divergence in trait-based assemblages driven by temperature zone-specific physicochemical conditions. Simultaneously, it is noteworthy that our data-driven multivariate analyses demonstrated pronounced heterogeneity in ciliate trait structures (including vertical distribution patterns, latitudinal dynamics, size spectrum, and biodiversity metrics) among five temperature zones (Figures 2–4). Among these, abiotic parameters, particularly temperature, likely played a significant role in driving these variations, as hypothesized (Chapin et al. 1997; Anderson et al. 2021; Tanioka et al. 2022; Jiao et al. 2024). Additionally, numerous scientific cruises in China have provided sampling opportunities spanning a latitudinal gradient of biological "hotspot" regions, which encompassing 175 sites (1117 samples) in the NFZ, SAZ, NTZ, TZ and SFZ. However, the current dataset remains geographically constrained, particularly lacking representation from Atlantic Ocean ecosystems where ciliate communities may exhibit distinct adaptive strategies. Hence, future research should prioritize comparative studies in Atlantic systems to test the global applicability of these findings.

and decoded that the dynamics of microzooplanktonic ciliate trait structures were governed by unique physicochemical feature in each temperature zone. Simultaneously, it is noteworthy that trait structures (including vertical distribution patterns, latitudinal dynamics, size spectrum, and species diversity) of ciliates, analyzed through a ground-based data-driven statistical approach, exhibited disproportionate variations among the five temperature zones mentioned (Figures 2-4). Among these, abiotic parameters, particularly temperature, likely played a significant role in driving these variations, as hypothesized (Chapin et al. 1997; Anderson et al. 2021; Tanioka et al. 2022; Jiao et al. 2024). Additionally, numerous scientific cruises in China have provided sampling opportunities spanning a latitudinal gradient of biological "hotspot" regions, which encompassing 175 sites in the NFZ, SAZ, NTZ, TZ and SFZ. However, it's essential to acknowledge that our study areas cannot fully represent the diverse adaptative strategies of ciliates across these regions, particularly in the Atlantic Ocean. Hence, further cruises and studies are necessary to conduct relevant experiments in the Atlantic Ocean in the near future.

4.1 Significant divergences in functional trait of ciliate size spectrum

Plankton size spectrum, which represents the distribution of individuals within a community or ecosystem by numerical abundance or biomass across size classes typically displayed on log axes, plays a crucial role in modulating various microbial processes, (e.g., carbon cycle driven by prey-predator interactions) such as the carbon cycle driven by prey-predator interactions (García-Comas et al. 2016; Andersen 2019; Trombetta et al. 2020; Serra-Pompei et al. 2022; Antoni et al. 2024; Atkinson et al. 2024),). Simultaneously, size spectrum provides insights into the ecological functions within marine food websand can elucidate ecological functions within marine food webs (Vandromme et al. 2012). In this sense, although empirical evidences has elucidated both the functional traits of plankton size spectra and valuable concurrent

带格式的: 字体: 10 磅

models,give details on both plankton size-spectra functional traits and concurrent valuable models, majority integrative analysis have primarily focused on biomass density within the size spectrum rather than on the abundance distribution across different trophic levelswere more dedicated to the biomass density size spectrum than their abundance amid different trophic levels (Sprules et al. 2016; Blanchard et al. 2017; Atkinson et al. 2024; Stukel et al. 2024). Currently, research on monospecific trophicspecific zooplankton groupassemblage, such as microzooplanktonic ciliates (Wang et al. 2024a), is rarely studied on a global scale. Similar to Stukel et al. (2024), our study revealed that the slopes of abundance size spectra in both the NFZ and SFZ were steeper in bipolar seas than other three regions latitudinally (Figure 3). Furthermore, the consistently steeper slopes at the surface compared to the 200 m layer across all regions (Figure 3) suggest: (1) a depth-dependent shift in pelagic ciliate community size structure, and (2) greater accessibility of prey for meso-/macro-zooplankton in surface waters compared to the 200 m layer, thereby influencing carbon flux efficiency to higher trophic levels (Stukel et al., 2024)the general trend of steeper slopes at the surface compared to the 200 m layer across all regions suggests a community size shift influencing carbon flux efficiency towards higher trophic levels (Stukel et al. 2024). In addition, Stukel et al. (2024) depicted that the slopes of the normalized biomass size spectra varied from −1.6 to −1.2 (median slope was −1.4) spanning over five orders of magnitude from phytoplankton to macrozooplankton in plankton communities in the tropical and subtropical seas. In contrast, our findings revealed the median slope was about −0.53 for the biomass size spectrum (no clear straight line on a log–-log plot) across all discrete depths of the global seas (Figure 3b4). We deem that the finer-scale monospecific trophic group, spanning one order of magnitude (10–-200 µm, microzooplankton), might be too small to accurately calculate the slopes of the normalized biomass size spectra (Sheldon et al. 1972). Conversely, it's noteworthy that the slopes of the abundance size spectrum exhibited an inverse relationship between abundance and body-size (Figure 3a), resembling the pyramid of numbers concept (Elton 1927; Trebilco et al. 2013; Blanchard et al. 2017). Hence, we posit that the slope of the abundance size spectrum may be more informative than its biomass counterpart in covering one order of magnitude within the plankton community. Moreover, the steeper slopes observed in the abundance size spectra in the bipolar seas compared to the tropical, temperate, and sub-Arctic seas might reflect a prevailing trend towards miniaturization (Li et al. 2009; Wang et al. 2023a).

4.2 Tintinnid biodiversity dynamics and its underlying formation mechanisms

By virtue of its critical role in regulating ecosystem processes and resource utilization efficiency, plankton species diversity play a crucial role in marine ecosystem functioning and biogeochemical cycling (Chapin et al. 1997). Similarly, a higher functionally similar species diversity enhances stability in resistance and resilience aspects of marine ecosystem processes (Ibarbalz et al. 2019; Benedetti et al. 2021; Chust et al. 2024). Consistent with both observational and modeling studies, tintinnid biodiversity was highest in the tropical and subtropical seas, and was lowest in the bipolar seas (Figure 45) (e.g., Sherr et al. 1997; Dolan et al. 2013, 2014, 2016; Righetti et al. 2019; Benedetti et al. 2021; Wang et al. 2019a, 2020, 2021, 2022b, 2024a; Li et al. 2016, 2018, 2022, 2023). Two explanations may account for this phenomenon. On one hand, the intrinsic mechanism is the endosymbiosis (Kutschera and Niklas 2005). After a long-term genetic DNA exchange and evolution process driven by closely prey-predation interaction (Chen et al. 2012), more diversified phytoplankton probable responsible for subsequent higher tintinnid biodiversity in tropical compared to bipolar zones through endosymbiosis mechanism (Margulis and Sagan 2002; Clark et al. 2023).

On the other hand, physical barriers constitute a fundamental extrinsic mechanism governing plankton biogeography~~represent an extrinsic mechanism~~ (Amargant-Arumí et al. 2024; Antoni et al. 2024; Chust et al. 2024). Generally, large-scale hydrographic features, particularly oceanic gyres and distinct water masses, create biogeographic discontinuities that disrupt ecological connectivity despite physical ocean connectivity (Yang et al. 2020). These mesoscale structures establish unique ecoregions with characteristic environmental sensitivities (Longhurst 2007), as evidenced by pronounced tintinnid community differentiation across the North Pacific Gyre, Subarctic Gyre, and Beaufort Gyre systems (Wang et al. 2020). Ultimately, elucidating biodiversity patterns across diverse temperature zones provides critical insights into microzooplankton adaptive affinity potential under climate change scenarios, particularly regarding niche conservation versus ecological plasticity in response to shifting oceanographic boundaries.

~~Biogeographically, the ecological connectivity of plankton biodiversity is hindered by large gyres or water masses within interconnected oceans (Yang et al. 2020), which are characterized by unique environmental sensitivities (Longhurst 2007). For instance, tintinnid species diversity exhibits distinct variations in the North Pacific Gyre, the Subarctic Gyre, and the Beaufort Gyre (Wang et al. 2020). Ultimately, understanding biodiversity dynamics across different temperature zones will benefit for studying the future adaptation mechanisms of microzooplankton in response to climate change.~~

4.3 Physicochemical factors determine the habitat of microzooplankton

Hydrography habitat conditions formed by large gyres (horizontal) or water masses (vertical) are critical factors in reshuffling sophisticated species composition of microbial food web (Lennartz et al. 2024). Conventionally, temperature can promote plankton biodiversity through regulating intrinsic temperature-dependent metabolic processes (Archibald et al. 2022; Lukić et al. 2022; Weisse 2024). Coincidentally, the statistically positive correlation observed between tintinnid species richness and temperature (Figure ~~7~~6) fully supports the abovementioned ecological process. In this perspective, we conclude that temperature determines organism mortality by affecting their thermal affinity within biogeochemical cycles (Knies et al., 2009; Stuart-Smith et al. 2015; Archibald et al., 2022; Chust et al. 2024) through an indirect effect (Weisse and Sonntag 2016; Weisse 2024). Similarly, through modulating osmotic pressure, salinity plays a crucial role in shaping the species composition of the microbial food web (Pedrós-Alió et al. 2000; Zang et al. 2024), and in hindering the dispersal of Pacific species into the Arctic Ocean (Wang et al. 2019b, 2022c). Our study, along with others, indicates that ciliate inhabiting higher salinity environments in both the TZ and NTZ (Figure ~~5~~S8) compared to bipolar regions might be a reflection of their higher osmotic pressure affinity.

Furthermore, the Chl *a* functionally serves as a critical ecological mediator in marine food webs, influencing ecosystem stability through both quantitative (abundance) and qualitative (polyunsaturated fatty acid composition) pathways via the fundamental prey-predator interplay (Šolić et al. 2010; Våge and Thingstad 2015; Holm et al. 2022). Consequently, Chl *a*

带格式的: 字体: 非倾斜

modulated the base of the energy flow of the entire marine ecosystem (Li et al. 2024). As direct micro-grazers of phytoplankton, both the abundance and species richness of ciliates exhibit a significant positive correlation with Chl *a* (Figure 6 and Figures S8– S10), aligning with the aforementioned viewpoint regarding the ecological role of Chl *a*. As outlined above, coupled with our results about multivariate analyses revealed strong hydrographic-ciliate relationships (Figure 6), while observed trait plasticity in ciliate communities (Yu et al. 2022) further supports the predominance of bottom-up control mechanisms (resource availability, prey quality) (Lu and Weisse 2022; Wang et al. 2023c, 2024c) over top-down regulation (predation pressure from microcrustaceans) (Power 1992; Calbet et al., 2001; Worm and Myers, 2003) in structuring global microzooplankton communities. This trophic cascade pattern underscores the fundamental role of primary production dynamics in governing ciliate population ecology across marine ecosystems.due to their ecological role in the fundamental prey-predator interplay, Chl *a* (food items for upper trophic levels) directly sustains the stability dynamics of marine ecosystems through both its quantity (abundance) and quality (content of unsaturated fatty acids) (Šolić et al. 2010; Våge and Thingstad 2015; Holm et al. 2022). Consequently, Chl *a* modulated the base of the entire marine ecosystem (Li et al. 2024). As direct micro-grazers of phytoplankton, both the abundance and species richness of ciliates exhibit a significant positive correlation with Chl *a* (Figure 5-7 and Figure S8), aligning with the aforementioned viewpoint regarding the ecological role of Chl *a*. As outlined above, considering the significant correlation between hydrographic factors and ciliates (abundance and species richness) (Figure 7), coupled with the trait structure of ciliate susceptible to environmental change (Yu et al. 2022), we conclude that bottom-up control (prey availability, resource limitation) (Lu and Weisse 2022; Wang et al. 2023c, 2024c) plays a primary role compared to top-down control (limited by microcrustacean predators or top grazer) (Power 1992; Calbet et al. 2001; Worm and Myers 2003) for microzooplanktonic ciliate in the global marine ecosystem.

4.4 Prediction for microzooplanktonic ciliate community to future global warming

Global warming, primarily stemming from anthropogenic industrial-induced CO_2 emissions, have caused enduring and irreversible impacts on marine ecosystems globally, impelling a suite of threats to biodiversity and marine ecosystem, such as phenology evolution and adaptation, species poleward dispersal and body-size miniaturization (Daufresne et al. 2009; Poloczanska et al. 2013; Atkinson et al. 2015; Hastings et al. 2020; Møller and Nielsen 2020; Yasumiishi et al. 2020; Wang and Wu 2022; Qian et al. 2023; Wang et al. 2024b). To date, contemporary biogeographic observations reveal marked increases in planktonic abundance and biodiversity across polar and subpolar seas (Ershova et al. 2015; Wassmann et al. 2015; Hunt et al. 2016; Kim et al. 2020; Lewis et al. 2020; Mueter et al. 2021; Wang et al. 2022a, 2023a), reflecting rapid thermal niche expansion under current warming regimes. Nevertheless, it should be mentioned that future global warming is expected to induce species extirpations by both compelling species beyond their thermal limits (Benedetti et al. 2021) and disrupting optimal survival habitats (Wang et al. 2024b).

existing facts indicate a significant increase in plankton abundance and species richness in bipolar and adjacent seas due to continuously rising temperature (Ershova et al. 2015; Wassmann et al. 2015; Hunt et al. 2016; Kim et al. 2020; Lewis et al.

带格式的: 下标

2020; Mueter et al. 2021; Wang et al. 2022a, 2023a) within a short timeframe. However, it should be mentioned that future global warming is expected to induce species extirpations by both compelling species beyond their thermal limits (Benedetti et al. 2021) and disrupting optimal survival habitats (Wang et al. 2024b).

Species poleward dispersal is another prominent aspect of plankton's responses to climate change (Hastings et al. 2020). Unfortunately, surface-dwelling ciliates (Kršinić 1982; Wang et al. 2019a, 2023a, 2024b) are particularly vulnerable to recent more frequent extreme temperature events, especially in tropical seas. Similarly, Benedetti et al. (2021) projected a median speed of approximately 35 km/decade for the poleward shift of species dispersal under a high CO_2 emission scenario by the end of this century. In this perspective, our study provides a fundamental benchmark for understanding the adaptive strategies (extirpation, dispersal, or adaptation) of ciliate to rapid warming processes in global seas. Meanwhile, unlike "winner" pioneer species possessing strong adaptation abilities (Casoli et al. 2020; Boutin et al. 2023), native species characterized by lower adaptive ability, such as the Arctic endemic tintinnid species *Ptychocylis urnula*, may either migrate passively to new environments (Wang et al. 2022a, 2023a, 2024b) or collapsed by a combination of warming and competition (Chust et al. 2024). Furthermore, the dynamics of future trophic food webs and biogeochemical flux in the global marine ecosystem will heavily rely on how indigenous and/or intrusive species adjust to a warmer ocean state amidst multiple ecosystem stressors.

带格式的: 下标

带格式的: 字体: 倾斜

5 Conclusions

Our results provides a comprehensive disparities in microzooplanktonic ciliate trait structure focused on size spectrum, biodiversity, and biotic-abiotic interplay based on 1117 water samples from 175 stations across five temperature zones from the North Pole to the Southern Ocean (Antarctic). Concerning ciliate size spectrum, slope of the normalized abundance value displayed an inverse relationship between ciliate abundance and body-size, resembling a pyramid norm, while the biomass-size spectrum showed relatively smoother slopes. Steeper ciliate abundance size spectra slopes in bipolar seas compared to tropical, temperate, and sub-Arctic seas suggest a prevalent trend of miniaturization. Additionally, tintinnid biodiversity was highest in tropical and subtropical seas and lowest in bipolar seas, likely influenced by endosymbiosis (intrinsic mechanism) and physical barriers (extrinsic mechanism). Furthermore, the interplay between biotic and abiotic factors manifested that temperature exert a primary influence on ciliate community structure. Under current foreseeable rapid global warming process, we conjecture that bottom-up control (resource limitation) playing a more primary role through an indireict way in the global marine ecosystem.

Acknowledgements

Special thanks to captains and crews of *R.V.* “Xuelong 2”, “Xiangyanghong ~~0~~1”, “Xiangyanghong ~~10~~6”, “Dongfanghong 3” and “Kexue” for their great help in sampling periods during the cruises. Meanwhile, we greatly appreciate the constructive comments by four anonymous reviewers for dramatically improving the quality of the manuscript.

Financial support

This research was supported by the National Natural Science Foundation of China (42206258), the Shandong Provincial Natural Science Foundation (ZR2022QD022), the National Natural Science Foundation of China (42276156; 42176228), and the International Research Project-Dynamics and Function of Marine Microorganisms (IRP-DYF2M): insight from physics and remote sensing, CNRS-CAS.

Competing interests

The contact author has declared that none of the authors has any competing interests.

References

Amargant-Arumí, M. Müller, O. Bodur, Y. Ntinou, I. Vonnahme, T. Assmy, P. Kohlbach, D. Chierici, M. Jones, E. Olsen, L. Tsagaraki, T. Reigstad, M. Bratbak, G. and Gradinger, R.: Interannual differences in sea ice regime in the north-western Barents Sea cause major changes in summer pelagic production and export mechanisms, Prog. Oceanogr. 220, 103178, doi:10.1016/j.pocean.2023.103178, 2024.

Andersen, K. H.: Chapter 2: Size spectrum theory. In Fish Ecology, Evolution, and Exploitation. A New Theoretical Synthesis (ed Andersen, K. H.). Princeton University Press. pp. 15–37, 2019.

Anderson, S. I. Barton, A. Clayton, S. Dutkiewicz, S. and Rynearson, T.: Marine phytoplankton functional types exhibit diverse responses to thermal change, Nat. Commun. 12, 6413, doi:10.1038/s41467-021-26651-8, 2021.

Antoni, J. Almandoz, G. Goldsmit, J. Garcia, M. FloresMelo, X. Hernando, M. and Schloss, I.: Long-term studies on West Antarctic Peninsula phytoplankton blooms suggest range shifts between temperate and polar species, Global Change Biol. 30, e17238, doi:10.1111/gcb.17238, 2024.

Archibald, K. M. Dutkiewicz, S. Laufkötter, C. and Moeller, H. V.: Thermal responses in global marine planktonic food webs are mediated by temperature effects on metabolism, J. Geophys. Res-Oceans 127, e2022JC018932, doi:10.1029/2022JC018932, 2022.

Atkinson, A. Harmer, R. Widdicombe, C. McEvoy, A. Smyth, T. Cummings, D. Somerfield, P. Maud, J. and Mcconville, K.: Questioning the role of phenology shifts and trophic mismatching in a planktonic food web, Prog. Oceanogr. 137, 498–512, doi:10.1016/j.pocean.2015.04.023, 2015.

Atkinson, A. Rossberg, A. G. Gaedke, U. Sprules, G. Heneghan, R. Batziakas, S. Grigoratou, M. Fileman, E. Schmidt, K. and Frangoulis, C.: Steeper size spectra with decreasing phytoplankton biomass indicate strong trophic amplification and future fish declines, Nat. Commun. 15, 381, doi:10.1038/s41467-023-44406-5, 2024.

Benedetti, F. Vogt, M. Elizondo, U. Righetti, D. Zimmermann, N. E. and Gruber, N.: Major restructuring of marine plankton assemblages under global warming, Nat. Commun. 12, 5226, doi:10.1038/s41467-021-25385-x, 2021.

Blanchard, J. L. Heneghan, R. F. Everett, J. D. Trebilco, R. and Richardson, A. J.: From bacteria to whales: Using functional size spectra to model marine ecosystems, Trends Ecol. Evol. 32, 174–186, doi:10.1016/j.tree.2016.12.003, 2017.

Boutin, K. Gaudron, S. M. Denis, J. and Lasram, F. B. R.: Potential marine benthic colonisers of offshore wind farms in the English Channel: a functional trait-based approach, Mar. Environ. Res. 190, 106061, doi:10.1016/j.marenvres.2023.106061, 2023.

Calbet, A. and Saiz, E.: The ciliate-copepod link in marine ecosystems, Aquat. Microb. Ecol. 38, 157–167, doi:10.3354/ame038157, 2005.

Calbet, A. Landry, M. and Nunnery, S.: Bacteria-flagellate interactions in the microbial food web of the oligotrophic subtropical North Pacific, Aquat. Microb. Ecol. 23, 283–292, doi:10.3354/ame023283, 2001.

Carvalho, K. S. Smith, T. E. and Wang, S.: Bering Sea marine heatwaves: Patterns, trends and connections with the Arctic, J. Hydrol. 600, 126462, doi:10.1016/j.jhydrol.2021.126462, 2021.

Casoli, E. Mancini, G. Ventura, D. Pace, D. S. Belluscio, A. and Ardizzone, G. D.: *Reteporella* spp. success in the re-colonization of bare coralligenous reefs impacted by Costa Concordia shipwreck: the pioneer species you did not expect, Mar. Pollut. Bull. 161, 111808, doi:10.1016/j.marpolbul.2020.111808, 2020.

Chapin III, F. S. Walker, B. H. Hobbs, R. J. Hooper, D. U. Lawton, J. H. Sala, O. E. and Tilman, D.: Biotic control over the functioning of ecosystems, Science 277, 500–503, doi:10.1126/science.277.5325.500, 1997.

Chen, B. Landry, M. R. Huang, B. and Liu, H.: Does warming enhance the effect of microzooplankton grazing on marine phytoplankton in the ocean?, Limnol. Oceanogr. 57, 519–526, doi:10.4319/lo.2012.57.2.0519, 2012.

Chust, G. Villarino, E. McLean, M. Mieszkowska, N. Benedetti-Cecchi, L. Bulleri, F. Ravaglioli, C. Borja, A. Muxika, I. Fernandes-Salvador, J.… and Lindegren, M.: Cross-basin and cross-taxa patterns of marine community tropicalization and deborealization in warming European seas, Nat. Commun. 15, 2126, doi:10.1038/s41467-024-46526-y, 2024.

Clark, M. S. Hoffman, J. Peck, L. S. Bargelloni, L. Gande, D. Havermans, C. Meyer, B. Patarnello, T. Phillips, T. Stoof-Leichsenring, K. … and Mock, T.: Multi-omics for studying and understanding polar life, Nat. Commun. 14, 7451, doi:10.1038/s41467-023-43209-y, 2023.

Darnis, G. Geoffroy, M. Dezutter, T. Aubry, C. Massicotte, P. Brown, T. Babin, M. Cote, D. and Fortier, L.: Zooplankton assemblages along the North American Arctic: Ecological connectivity shaped by ocean circulation and bathymetry from the Chukchi Sea to Labrador Sea, Elementa-Sci. Anthrop. 10, 1, doi:10.1525/elementa.2022.00053, 2022.

Daufresne, M. Lengfellner, K. and Sommer, U.: Global warming benefits the small in aquatic ecosystems, P. Natl. Acad. Sci. USA. 106, 12788–12793, doi:10.1073/pnas.0902080106, 2009.

Dolan, J. R. and Pierce, R. W.: Diversity and distributions of tintinnid ciliates. In: Dolan, J. R., Agatha, S., Coats, D. W. (Eds.), The Biology and Ecology of Tintinnid Ciliates: Models for Marine Plankton. Wiley-Blackwell, Oxford, pp. 214–243, 2013.

Dolan, J. R. Vidussi, F. and Claustre, H.: Planktonic ciliates in the Mediterranean Sea: longitudinal trends, Deep-Sea Res. I. 46, 2025–2039, doi:10.1016/S0967-0637(99)00043-6, 1999.

Dolan, J. R. Yang, E. J. Kang, S. H. and Rhee, T. S.: Declines in both redundant and trace species characterize the latitudinal diversity gradient in tintinnid ciliates, ISME J. 10, 2174–2183, doi:10.1038/ismej.2016.19, 2016.

Dolan, J. R. Yang, E. J. Kim, T. W. and Kang, S. H.: Microzooplankton in warming Arctic: a comparison of tintinnids and radiolarians from summer 2011 and 2012 in the Chukchi Sea, Acta Protozool. 52, 101–113, doi:10.4467/16890027AP.14.010.1447, 2014.

Dolan, J. R. Yang, E. J. Lee, S. H. and Kim, S. Y.: Tintinnid ciliates of Amundsen Sea (Antarctica) plankton communities, Polar Res. 32, 19784, doi:10.3402/polar.v32i0.19784, 2013.

du Pontavice, H. Gascuel, D. Reygondeau, G. Stock, C. and Cheung, W.: Climate–induced decrease in biomass flow in marine food webs may severely affect predators and ecosystem production, Global Change Biol. 11, 2608–2622, doi:10.1111/gcb.15576, 2021.

Elton, C.: Animal ecology. Macmillan, New York, 1927.

Ershova, E. A. Hopcroft, R. Kosobokova, K. Matsuno, K. Nelson, R. Yamaguchi, A. and Eisner, L.: Long-term changes in summer zooplankton communities of the western Chukchi Sea, 1945–2012, Oceanography 28, 100–115, doi:10.5670/oceanog.2015.60, 2015.

García-Comas, C. Sastri, A. R. Ye, L. Chang, C. Y. Lin, F. Su, M. Gong, G. and Hsieh, C. H.: Prey size diversity hinders biomass trophic transfer and predator size diversity promotes it in planktonic communities, P. Roy. Soc. B-Biol. Sci. 283, 20152129, doi:10.1098/rspb.2015.2129, 2016.

Gómez, F.: Trends on the distribution of ciliates in the open Pacific Ocean, Acta Oecol. 32, 188–202, doi:10.1016/j.actao.2007.04.002, 2007.

Hastings, R. A. Rutterford, L. A. Freer, J. J. Collins, R. A. Simpson, S. D. and Genner, M. J.: Climate change drives poleward increases and equatorward declines in marine species, Curr. Biol. 30, 1572–1577, doi:10.1016/j.cub.2020.02.043, 2020.

Heneghan, R. F. Everett, J. D. Blanchard, J. L. Sykes, P. and Richardson, A. J.: Climate-driven zooplankton shifts cause large-scale declines in food quality for fish, Nat. Clim. Change 13, 470–477, doi:10.1038/s41558-023-01630-7, 2023.

Hillman, J. R. Lundquist, C. J. and Thrush, S. F.: The challenges associated with connectivity in ecosystem processes, Front. Mar. Sci. 5, 364, doi:10.3389/fmars.2018.00364, 2018.

Holm, H. C. Fredricks, H. F. Bent, S. M. Lowenstein, D. P. Ossolinski, J. E. Becker, K. W. Johnson, W. M. Schrage, K. and Van Mooy, B.: Global Ocean lipidomes show a universal relationship between temperature and lipid unsaturation, Science 376, 1487–1491, doi:10.1126/science.abn7455, 2022.

Hunt, G. L. Drinkwater, K. F. Arrigo, K. Berge, J. Daly, K. L. Danielson, S. Daase, M. Hop, H. Isla, E. Karnovsky, N. … and Wolf-Gladrow, D.: Advection in polar and sub-polar environments: Impacts on high latitude marine ecosystems, Prog. Oceanogr. 149, 40–81, doi:10.1016/j.pocean.2016.10.004, 2016.

Ibarbalz, F. Henry, N. Brandão, M. Martini, S. Busseni, G. Byrne, H. Coelho, L. P. Endo, H. Gasol, J. Gregory, A. … and Sabrina, S.: Global trends in marine plankton diversity across kingdoms of life, Cell 179, 1084–1097, doi:10.1016/j.cell.2019.10.008, 2019.

IPCC.: Climate Change 2023: Synthesis Report. Contribution of Working Groups I, II and III to the Sixth Assessment Report of the Intergovernmental Panel on Climate Change. IPCC, Geneva, Switzerland. pp.1–169, 2023.

Jiang, Y. Yang, E. Min, J. Kang, S. and Lee, S.: Using pelagic ciliated microzooplankton communities as an indicator for monitoring environmental condition under impact of summer sea-ice reduction in western Arctic Ocean, Ecol. Indic. 34, 380–390, doi:10.1016/j.ecolind.2013.05.026, 2013.

Jiao, N. Luo, T. Chen, Q. Zhao, Z. Xiao, X. Liu, J. Jian, Z. Xie, S. Thomas, H. Herndl, G. … and Robinson, C.: The microbial carbon pump and climate change, Nat. Rev. Microbiol. 1–12, doi:10.1038/s41579-024-01018-0, 2024.

Kato, S. and Taniguchi, A.: Tintinnid ciliates as indicator species of different water masses in the western North Pacific Polar Front, Fish. Oceanogr. 2, 166–174, doi:10.1111/j.1365-2419.1993.tb00132.x, 1993.

Kim, J. H. Cho, K. H. La, H. S. Choy, E. J. and Yang, E. J.: Mass occurrence of Pacific copepods in the southern Chukchi Sea during summer: implications of the high-temperature Bering Summer Water, Front. Mar. Sci. 7, 612, doi:10.3389/fmars.2020.00612, 2020.

Knies, J. Kingsolver, J. and Burch, C. Hotter is better and broader: Thermal sensitivity of fitness in a population of bacteriophages. Am. Nat. 173, 419–430, doi:10.1086/597224, 2009.

Kohlbach, D. Goraguer, L. Bodur, Y. V. Müller, O. Amargant-Arumí, M. Blix, K. Bratbak, G. Chierici, M. Dabrowska, A. M. Dietrich, U. … and Assmy, P.: Earlier sea-ice melt extends the oligotrophic summer period in the Barents Sea with low algal biomass and associated low vertical flux, Prog. Oceanogr. 213, 103018, doi:10.1016/j.pocean.2023.103018, 2023.

Köppen, W. P.: The geographical system of climates (Das geographische system der klimate). In Handbook of climatology (Handbuch der klimatologie), ed. W. P. Köppen, and R. Geiger, 1–44. Berlin: Gebrüder Borntraeger, 1936.

Kršinić, F.: On vertical distribution of tintinnines (Ciliata, Oligotrichida, Tintinnina) in the open waters of the South Adriatic, Mar. Biol. 68, 83–90, doi:10.1007/BF00393145, 1982.

Kutschera, U. and Niklas, K. J.: Endosymbiosis, cell evolution, and speciation, Theor. Biosci. 124, 1–24, doi:10.1016/j.thbio.2005.04.001, 2005.

Kwiatkowski, L. Aumont, O. and Bopp, L.: Consistent trophic amplification of marine biomass declines under climate change, Global Change Biol. 25, 218–229, doi:10.1111/gcb.14468, 2019.

Lennartz, S. T. Keller, D. P. Oschlies, A. Blasius, B. and Dittmar, T.: Mechanisms underpinning the net removal rates of dissolved organic carbon in the global ocean, Global Biogeochem. Cy. 38, e2023GB007912, doi:10.1029/2023GB007912, 2024.

Lewis, K. M. Van Dijken, G. L. and Arrigo, K. R.: Changes in phytoplankton concentration now drive increased Arctic Ocean primary production, Science 369, 198–202, doi:10.1126/science.aay8380, 2020.

Li, C. Chen, K. Sun, X. Liu, L. Ming, X. Liu, X. and Wang, B.: Summer sea ice melting enhances phytoplankton and dimethyl sulfide production. Limnol. Oceanogr. 69, 2453–2472, doi:10.1002/lno.12681, 2024.

Li, H. Xu, Z. Zhang, W. Wang, S. Zhang, G. and Xiao, T.: Boreal tintinnid assemblage in the Northwest Pacific and its connection with the Japan Sea in summer 2014. PLoS One 11, e0153379, doi:10.1371/journal.pone.0153379, 2016.

Li, H. Zhang, W. Zhao, Y. Zhao, L. Dong, Y. Wang, C. Liang, C. and Xiao, T.: Tintinnid diversity in the tropical West Pacific Ocean, Acta Oceanol. Sin. 37, 218–228, doi:10.1007/s13131-018-1148-x, 2018.

Li, H. Xu, Z. Mou, W. Gao, L. Zu, Y. Wang, C. Zhao, Y. Zhang, W. and Xiao, T.: Planktonic ciliates in different water masses of Cosmonaut and Cooperation Seas (Indian sector of the Southern Ocean) during austral summer, Polar Biol. 45, 1059–1076, doi:10.1007/s00300-022-03057-w, 2022.

Li, W. Mclaughlin, F. A. Lovejoy, C. and Carmack, E. C.: Smallest algae thrive as the Arctic Ocean freshens, Science 326, 539–539, doi:10.1126/science.1179798, 2009.

Longhurst, A. R.: Ecological Geography of the Sea. 2nd ed. Amsterdam: Academic Press, 2007.

Lotze, H. K. Tittensor, D. P. Bryndum-Buchholz, A. Eddy, T. D. Cheung, W. Galbraith, E. D. Barange, M. Barrier, N. Bianchi, D. Blanchard, J. L. … and Worm, B.: Global ensemble projections reveal trophic amplification of ocean biomass declines with climate change, P. Natl. Acad. Sci. USA. 116, 12907–12912, doi:10.1073/pnas.1900194116, 2019.

Lukić, D. Limberger, R. Agatha, S. Montagnes, D.J. and Weisse. T.: Thermal performance of planktonic ciliates differs between marine and freshwaters: A case study providing guidance for climate change studies. Limnol. Oceanogr. Lett. 7, 520–526, doi:10.1002/lol2.10264, 2022.

Lu, X. and Weisse, T.: Top-down control of planktonic ciliates by microcrustacean predators is stronger in lakes than in the ocean, Sci. Rep. 12, 10501, doi:10.1038/s41598-022-14301-y, 2022.

Lynn, D. H.: Ciliated Protozoa: Characterization, Classification, and Guide to the Literature, third ed. Springer, Berlin. pp. 1–455, 2008.

Margalef, R.: Information theory in ecology, Gen. Syst. 3, 36–71, 1958.

Margulis, L. and Sagan, D.: Acquiring Genomes. A theory of the origin of species. Basic Books, New York, 2002.

Møller, E. F. and Nielsen, T. G.: Borealization of Arctic zooplankton–smaller and less fat zooplankton species in Disko Bay, Western Greenland, Limnol. Oceanogr. 65, 1175–1188, doi:10.1002/lno.11380, 2020.

Mueter, F. J. Iken, K. Cooper, L. Grebmeier, J. M. Kuletz, K. J. Hopcroft, R. R. Danielson, S. Collins, R. and Cushing, D.: Changes in diversity and species composition across multiple assemblages in the eastern Chukchi Sea during two contrasting years are consistent with borealization, Oceanography 34, 38–51, doi:10.5670/oceanog.2021.213, 2021.

Neukermans, G. Oziel, L. and Babin, M.: Increased intrusion of warming Atlantic water leads to rapid expansion of temperate phytoplankton in the Arctic, Global Change Biol. 24, 2545–2553, doi:10.1111/gcb.14075, 2018.

Noh, K. M. Oh, J. H. Lim, H. G. Song, H. and Kug, J. S.: Role of Atlantification in enhanced primary productivity in the Barents Sea, Earth's Future 12, e2023EF003709, doi:10.1029/2023EF003709, 2024.

Oziel, L. Baudena, A. Ardyna, M. Massicotte, P. Randelhoff, A. Sallée, J. B. Ingvaldsen, R. B. Devred, E. and Babin, M.: Faster Atlantic currents drive poleward expansion of temperate phytoplankton in the Arctic Ocean, Nat. Commun. 11, 1–8, doi:10.1038/s41467-020-15485-5, 2020.

Pedrós-Alió, C. Calderón-Paz, J. I. MacLean, M. H. Medina, G. Marrasé, C. Gasol, J. M. and Guixa-Boixereu, N.: The microbial food web along salinity gradients, FEMS Microbiol. Ecol. 32, 143–155, doi:10.1111/j.1574-6941.2000.tb00708.x, 2000.

Pierce, R. W. and Turner, J. T.: Global biogeography of marine tintinnids, Mar. Ecol. Prog. Ser. 94, 11–26, doi:10.3354/meps094011, 1993.

Poloczanska, E. Brown, C. Sydeman, W. Kiessling, W. Schoeman, D. Moore, P. Brander, K. Bruno, J. Buckley, L. Burrows, M. … and Richardson, A.: Global imprint of climate change on marine life, Nat. Clim. Change 3, 919–925, doi：10.1038/NCLIMATE1958, 2013.

Power, M. E.: Top-down and bottom-up forces in food webs: do plants have primacy. Ecology 73, 733–746, doi:10.2307/1940153, 1992.

Putt, M. and Stoecker, D. K.: An experimentally determined carbon: volume ratio for marine "oligotrichous" ciliates from estuarine and coastal waters. Limnol. Oceanogr. 34, 1097–1103, doi:10.4319/lo.1989.34.6.1097, 1989.

Qian, C. Liu, K. Pang, M. Xu, Z. Deng, L. and Liu, H.: Hypoxia and warming take sides with small marine protists: An integrated laboratory and field study, Sci. Total Environ. 882, 163568, doi:10.1016/j.scitotenv.2023.163568, 2023.

Righetti, D. Vogt, M. Gruber, N. Psomas, A. and Zimmermann, N. E.: Global pattern of phytoplankton diversity driven by temperature and environmental variability, Sci. Adv. 5, eaau6253, doi:10.1126/sciadv.aau6253, 2019.

Screen, J. A., and Simmonds, I.: The central role of diminishing sea ice in recent Arctic temperature amplification, Nature 464, 1334–1337, doi:10.1038/nature09051, 2010.

Segaran, T.C. Azra, M. Lananan, F. and Wang, Y.: Microbe, climate change and marine environment: Linking trends and research hotspots, Mar. Environ. Res. 189, 106015, doi:10.1016/j.marenvres.2023.106015, 2023.

Serra-Pompei, C. Ward, B. Pinti, J. Visser, A. Kiorboe, T. and Andersen, K.: Linking plankton size spectra and community composition to carbon export and its efficiency, Global Biogeochem. Cy. 36, e2021GB007275, doi:10.1029/2021GB007275, 2022.

Serreze, M. Barrett, A. Stroeve, J. Kindig, D. and Holland, M.: The emergence of surface-based Arctic amplification, Cryosphere 3, 11–19, doi:10.5194/tc-3-11-2009, 2009.

Shannon, C. E.: A mathematical theory of communication, Bell System Technical Journal 27, 379–423, doi:10.1002/j.1538-7305.1948.tb01338.x, 1948.

Sheldon, R. W. Prakash, A. Sutcliffe, W.: The size distribution of particles in the ocean, Limnol. Oceanogr. 17, 327–340, doi:10.4319/lo.1972.17.3.0327, 1972.

Sherr, E. B. Sherr, B. F. and Fessenden, L.: Heterotrophic protists in the central Arctic Ocean, Deep-Sea Res. II 44, 1665–1673, doi:10.1016/S0967-0645(97)00050-7, 1997.

Šolić, M. Krstulović, N. Kuspilić, G. Gladan, N. Bojanić, N. Sestanovic, S. Šantić, D. and Ordulj, M.: Changes in microbial food web structure in response to changed environmental trophic status: A case study of the Vranjic Basin (Adriatic Sea), Mar. Environ. Res. 70, 239–49, doi:10.1016/j.marenvres.2010.05.007, 2010.

Spalding, M. Agostini, V. Rice, J. and Grant, S.: Pelagic provinces of the world: A biogeographic classification of the world's surface pelagic waters. Ocean Coast. Manage. 60, 19–30, doi:10.1016/j.ocecoaman.2011.12.016, 2012.

Sprules, W. G. Barth, L. E. and Giacomini, H.: Surfing the biomass size spectrum: some remarks on history, theory, and application, Can. J. Fish. Aquat. Sci. 73, 477–495, doi:10.1139/cjfas-2015-0115, 2016.

Stabeno, P. J. Farley-Jr, E. Kachel, N. Moore, S. Mordy, C. Napp, J. Overland, J. Pinchuk, A. and Sigler, M.: A comparison of the physics of the northern and southern shelves of the eastern Bering Sea and some implications for the ecosystem, Deep-Sea Res. II 65–70, 14–30, doi:10.1016/j.dsr2.2012.02.019, 2012.

Stoecker, D. K. Michaels, A. and Davis, L.: Grazing by the jellyfish, *Aurelia aurita*, on microzooplankton, J. Plankton Res. 9, 901–915, doi:10.1093/plankt/9.5.901, 1987.

Strom, S. L. and Fredrickson, K. A.: Intense stratification leads to phytoplankton nutrient limitation and reduced microzooplankton grazing in the southeastern Bering Sea, Deep-Sea Res. II 55, 1761–1774, doi:10.1016/j.dsr2.2008.04.008, 2008.

Stuart-Smith, R. D. Edgar, G. Barrett, N. Kininmonth, S. and Bates, A.: Thermal biases and vulnerability to warming in the world's marine fauna, Nature 528, 88–92, doi:10.1038/nature16144, 2015.

Stukel, M. Décima, M. Kelly, T. Landry, M. Nodder, S. Ohman, M. Selph, K. and Yingling, N.: Relationships between plankton size spectra, net primary production, and the biological carbon pump, Global Biogeochem. Cy. 38, e2023GB007994, doi:10.1029/2023GB007994, 2024.

Tagliabue, A. Twining, B. Barrier, N. Maury, O. Berger, M. and Bopp, L.: Ocean iron fertilization may amplify climate change pressures on marine animal biomass for limited climate benefit, Global Change Biol. 29, 5250–5260, doi:10.1111/gcb.16854, 2023.

Taniguchi, A.: Microzooplankton biomass in Arctic and subarctic Pacific Ocean in summer, Mem. Natl. Inst. Polar Res. Spec. Issue 32, 63–80, 1984.

Tanioka, T. Garcia, C. Larkin, A. Garcia, N. Fagan, A. and Martiny, A.: Global patterns and predictors of C:N:P in marine ecosystems, Commun. Earth Environ. 3, 271, doi:10.1038/s43247-022-00603-6, 2022.

Tittensor, D. P. Novaglio, C. Harrison, C. Heneghan, R. Barrier, N. Bianchi, D. Bopp, L. Bryndum-Buchholz, A. Britten, G. Büchner, M. … and Blanchard, J.: Next-generation ensemble projections reveal higher climate risks for marine ecosystems, Nat. Clim. Change 11, 973–981, doi:10.1038/s41558-021-01173-9, 2021.

Trebilco, R. Baum, J. K. Salomon, A. K. and Dulvy, N. K.: Ecosystem ecology: size-based constraints on the pyramids of life. Trends Ecol. Evol. 28, 423–431, doi:10.1016/j.tree.2013.03.008.PMID:23623003, 2013.

Trewartha, G. T. Robinson, A. H. and Hammond, E. H.: The Physical Elements of Geography. In: The Elements of Weather and Climate, 24. New York: McGraw-Hill Book Company, 1967.

Trombetta, T. Vidussi, F. Roques, C. Scotti, M. and Mostajir, B.: Marine microbial food web networks during phytoplankton bloom and non-bloom periods: Warming favors smaller organism interactions and intensifies trophic cascade. Front. Microbiol. 11, 502336, doi:10.3389/fmicb.2020.502336, 2020.

Utermöhl, H.: Zur vervollkommnung der quantitativen phytoplankton Methodik, Mit. Int. Ver. Theor. Angew. Limnol. 9, 1–38, 1958.

Våge, S. and Thingstad, T. F.: Fractal hypothesis of the pelagic microbial ecosystem –can simple ecological principles lead to self-similar complexity in the pelagic microbial food web?, Front. Microbiol. 6, 1357, doi:10.3389/fmicb.2015.01357, 2015.

Vandromme, P. Stemmann, L. García-Comas, C. Berline, L. Sun, X. and Gorsky, G.: Assessing biases in computing size spectra of automatically classified zooplankton from imaging systems: A case study with the ZooScan integrated system, Methods in Oceanography 1, 3–21, doi:10.1016/j.mio.2012.06.001, 2012.

Verberk, W. Atkinson, D. Hoefnagel, K. Hirst, A. Horne, C. and Siepel, H.: Shrinking body sizes in response to warming: explanations for the temperature–size rule with special emphasis on the role of oxygen, Biol. Rev. 96, 247–268, doi:10.1111/brv.12653, 2021.

Verity, P. and Lagdon, C.: Relationships between lorica volume, carbon, nitrogen, and ATP content of tintinnids in Narragansett Bay, J. Plankton Res. 6, 859–868, doi:10.1093/plankt/6.5.859, 1984.

Wang, C. Li, H. Zhao, L. Zhao, Y. Dong, Y. Zhang, W. and Xiao, T.: Vertical distribution of planktonic ciliates in the oceanic and slope areas of the western Pacific Ocean, Deep-Sea Res. II 167, 70–78, doi:10.1016/j.dsr2.2018.08.002, 2019a.

Wang, C. Xu, Z. Liu, C. Li, H. Liang, C. Zhao, Y. Zhang, G. Zhang, W. and Xiao, T.: Vertical distribution of oceanic tintinnid (Ciliophora: tintinnida) assemblages from the Bering sea to Arctic Ocean through Bering Strait, Polar Biol. 42, 2105–2117, doi:10.1007/s00300-019-02585-2, 2019b.

Wang, C. Li, H. Xu, Z. Zheng, S. Hao, Q. Dong, Y. Zhao, L. Zhang, W. Zhao, Y. and Xiao, T.: Difference of planktonic ciliate communities of the tropical West Pacific, the Bering Sea and the Arctic Ocean, Acta Oceanol. Sin. 39, 9–17, doi:10.1007/s13131-020-1541-0, 2020.

Wang, C. Xu, M. Xuan, J. Li, H. Zheng, S. Zhao, Y. Zhang, W. and Xiao, T.: Impact of the warm eddy on planktonic ciliate, with an emphasis on tintinnids as bioindicator species, Ecol. Indic. 133, 108441, doi:10.1016/j.ecolind.2021.108441, 2021.

Wang, C. Wang, X. Xu, Z. Hao, Q. Zhao, Y. Zhang, W. and Xiao, T.: Planktonic tintinnid community structure variations in different water masses of the Arctic Basin, Front. Mar. Sci. 8, 775653, doi:10.3389/fmars.2021.775653, 2022a.

Wang, C. Zhao, Y. Du, P. Ma, X. Li, S. Li, H. Zhang, W. and Xiao, T.: Planktonic ciliate community structure and its distribution in the oxygen minimum zones in the Bay of Bengal (eastern Indian Ocean), J. Sea Res. 190, 102311, doi:10.1016/j.seares.2022.102311, 2022b.

Wang, C. Yang, M. He, Y. Xu, Z. Zhao, Y. Zhang, W. and Xiao, T.: Hydrographic feature variation caused pronounced differences of planktonic ciliate community in the Pacific Arctic Region in summer 2016 and 2019, Front. Microbiol. 13, 881048, doi:10.3389/fmicb.2022.881048, 2022c.

Wang, C. Wang, X. Xu, Z. Luo, G. Chen, C. Li, H. Liu, Y. Li, J. He, J. Chen, H. and Zhang, W.: Full-depth vertical distribution of planktonic ciliates (Ciliophora) and a novel bio-index for indicating habitat suitability of tintinnid in the Arctic Ocean, Mar. Environ. Res. 186, 105924, doi:10.1016/j.marenvres.2023.105924, 2023a.

Wang, C. Wang, X. Wei, Y. Guo, G. Li, H. Wan, A. and Zhang, W.: Pelagic ciliate (Ciliophora) communities in the Southern Ocean: bioindicator to water mass, habitat suitability classification and potential response to global warming, Prog. Oceanogr. 216, 103081, doi:10.1016/j.pocean.2023.103081, 2023b.

Wang, C. Zhao, L. Wei, Y. Xu, Z. Zhao, Y. Zhao, Y. Zhang, W. and Xiao, T. Insights into the structure of the pelagic microbial food web in the oligotrophic tropical Western Pacific: Examining trophic interactions and relationship with abiotic variables, Mar. Pollut. Bull. 197, 115772, doi:10.1016/j.marpolbul.2023.115772, 2023c.

Wang, C. Xu, Z. Wang, X. He, Y. Xu, Z. Luo, G. Li, H. Chen, X. and Zhang, W.: Insights into the pelagic ciliate community in the Bering Sea: Carbon stock, driving factors and indicator function for climate change, J. Marine Syst. 244, 103975, doi:10.1016/j.jmarsys.2024.103975, 2024a.

Wang, C. Xu, Z. Wan, A. Wang, X. Luo, G. Bian, W. Chen, Q. Chen, X. and Zhang, W.: Diatom bloom trigger notable variations in microzooplanktonic ciliate composition, body-size spectrum and biotic-abiotic interaction in the Arctic Ocean, Environ. Res. 252, 118821, doi:10.1016/j.envres.2024.118821, 2024b.

Wang, C. Zhao, C. Zhou, B. Xu, Z. Ma, J. Li, H. Wang, W. Chen, X. and Zhang, W.: Latitudinal pronounced variations in tintinnid (Ciliophora) community at surface waters from the South China Sea to the Yellow Sea: Oceanic-to-neritic species shift, biotic-abiotic interaction and future prediction, Sci. Total Environ. 912, 169354, doi:10.1016/j.scitotenv.2023.169354, 2024c.

Wang, Y. and Wu, C.: Rapid surface warming of the Pacific Asian Marginal Seas since the late 1990s, J. Geophys. Res-Oceans 127, c2022JC018744, doi:10.1029/2022JC018744, 2022.

Wassmann, P. Kosobokova, K. Slagstad, D. Drinkvvater, K. Hoperoft, R. Moore, S. Ellingsen, I. Nelson, R. Carmack, E. Popova, E. and Berge, J.: The contiguous domains of Arctic Ocean advection: Trails of life and death, Prog. Oceanogr. 139, 42–65, doi:10.1016/j.pocean.2015.06.011, 2015.

Weisse, T.: Physiological mortality of planktonic ciliates: Estimates, causes, and consequences, Limnol. Oceanogr. 69, 524–532, doi:10.1002/lno.12503, 2024.

Weisse, T. and Sonntag, B.: Ciliates in Planktonic Food Webs: Communication and Adaptive Response. In: Witzany, G., Nowacki, M. (eds) Biocommunication of Ciliates. Springer, Cham, 2016.

Worm, B. and Myers, R.: Meta-analysis of cod-shrimp interactions reveals top-down control in oceanic food webs, Ecology 84, 162–173, doi:10.1890/0012-9658(2003)084[0162:MAOCSI]2.0.CO;2, 2003.

Yang, E. J. Lee, Y. and Lee, S.: Trophic interactions of micro- and mesozooplankton in the Amundsen Sea polynya and adjacent sea ice zone during austral late summer, Prog. Oceanogr. 174, 117–130, doi:10.1016/j.pocean.2018.12.003, 2019.

Yang, H. Lohmann, G. Krebs-Kanzow, U. Ionita, M. Shi, X. Sidorenko, D. Gong, X. Chen, X. and Gowan E. J.: Poleward shift of the major ocean gyres detected in a warming climate, Geophys. Res. Lett. 47, e2019GL085868, doi:10.1029/2019GL085868, 2020.

Yasumiishi, E. M. Cieciel, K. Andrews, A. Murphy, J. and Dimond, J.: Climate-related changes in the biomass and distribution of small pelagic fishes in the eastern Bering Sea during late summer, 2002–2018, Deep-Sea Res. II 181–182, 104907, doi:10.1016/j.dsr2.2020.104907, 2020.

Yu, X. Li, X. Liu, Q. Yang, M. Wang, X. Guan, Z. Yang, J. Liu, M. Yang, E. and Jiang, Y.: Community assembly and co-occurrence network complexity of pelagic ciliates in response to environmental heterogeneity affected by sea ice melting in the Ross Sea, Antarctica, Sci. Total Environ. 836, 155695, doi:10.1016/j.scitotenv.2022.155695, 2022.

Zang, L. Liu, Y. Jiao, N. Zhong, K. Song, X. Yang, Y. Cai, L. Liu, K. Mao, G. Ji, M. and Zhang, R.: Salinity as a key factor affecting viral activity and life strategies in alpine lakes, Limnol. Oceanogr. 69, 961–975, doi:10.1002/lno.12540, 2024.

Zhang, W. Feng, M. Yu, Y. Zhang, C. and Xiao, T.: An illustrated guide to contemporary tintinnids in the world. Science Press, Beijing. pp. 1–499, 2012.